In-situ Adhesive Strength Study of "Oilygel"

Submitted By
Matthew F. Glenn

IN PARTIAL FULFILLMENT OF THE REQUIREMENTS FOR THE DEGREE
OF
BACHELOR OF SCIENCE IN MECHANICAL ENGINEERING

School Of Engineering
Tufts University
Medford, Massachusetts

May 2011

ABSTRACT

In-situ Adhesive Strength Study of "Oilygel"

By

Matthew F. Glenn

With the recent rise in offshore oil exploration there had been a demand for a safe and easily

deployable method of oil well containment in the event of blowouts and other emergencies.   In

response to this call *Aspen Aerogel* has developed "oilygel." A byproduct of a chemical

reaction, "oilygel" forms a semi rigid gel. This gel has exhibited many useful characteristics

among which are a high cohesive strength, the ability to solidify in the presence of hydrocarbons,

and adhesive properties. To determine the viability of "oilygel" as a successful containment

method a rig has been constructed to simulate an oil well cross section and allow for the

determination of the adhesive strength of the "oilygel" as a function of surface area. This rig has

shown that the "oilygel's" adhesive strength increases monotonically as a function of sample

length. As the diameter of oil production casing is more or less constant the diameter of these

samples was held constant to maintain the validity of the experiment. By developing an adhesive

strength correlation for the "oilygel" it was then possible to determine the appropriate length of

the "oilygel" necessary to effectively contain a renegade oil well. Based on a 25.4 mm cross

section and a typical formation pressure of 32.06 MPa this experiment showed that the "oilygel"

plug would need to be 100.17 m in length. For a typical production casing with a diameter of

around 127 mm this length would need to be around 1604.4 m. However, adhesive strength had

been shown to increase with the width of the adhered area so this length could be appreciably

shorter. Regardless this length is within reason given that typical well bores extend more than 3218 m into the ground.

ACKNOWLEDGEMENTS

Table of Contents

Nomenclature

H	pressure head
P_R	reservoir pressure
ρ_D	density of drilling fluid
g	gravitational constant
F_T	shear load
L_C	length of concrete plug
τ	average shear stress
d_W	well diameter
τ_a	actual shear stress
V_d	Van der Waals potential energy
A_S	interacting surface are of the plates
A	Hamaker Constant
z	seperation of the plates
h_1	thickness of plate 1
h_2	thickness of plate 2
F_D	Van der Waals interaction force
∇	gradient
F_A	measuresed applied force
D	diameter of test section
L	experimental length of oilygel specimen
$P(L)$	compressive stress as a funtion of specimen length

List of Figures

1. Introduction & Background

"Oilygel" is a concept envisioned by *Aspen Aerogels* as a method of rapidly containing renegade oil wells. "Oilygel" exhibits a number of useful properties that made it suitable for this application. Specifically it has a very short curing time of less than thirty seconds, strong internal cohesion, adhesive qualities, and an inert hydrocarbon constituent. Combined these characteristics of "oilygel" imply that it may be possible to create a cohesive semi-rigid gel plug of the "oilygel" in an uncontrolled hydrocarbon flow. Given its fast curing time it is possible that the "oilygel" would be able to form adhesive bonds with the oil well production casing and resist the flow of oil. The objective of the work presented in this thesis was to determine the strength of the "oilygel's" adhesive bonds to access the viability of the product as a means of containing rogue oil wells.

1.1 Oil Well Blowouts and Containment Methods

With the continued advancement of offshore oil exploration a number of methods have been devised to contain or "kill" wells that have begun to release oil in an uncontrolled fashion due to mechanical or structural failure of oil well components [1]. Commonly these situations are the result of a "kick", or pressure surge, caused by drilling into a high pressure formation without a proper amount of hydrostatic pressure on the formation which causes a mechanical or structural failure in the well. This hydrostatic pressure is usually maintained through the use of drilling fluids such as emulsified fluids. Although many species of these fluids exist, those most widely in use in the oil exploration field are either oil in a water base or water in an oil base. The two fluids are emulsified using a surfactant that allows for the reduction in the interfacial tension of the fluids being mixed [1]. Using this combination it is possible to modify the density of the fluid in order to account for higher formation pressures.

In an uncontrolled well situation there are a number of procedures used to balance the formation pressure using these fluids. These methods involve pumping the kill fluids into the well bore in order to displace the lighter fluid and increase the hydrostatic pressure over the formation and reduce the pressure experienced near the top of the well [1]. By reducing the pressure in the upper section of the well bore it is then possible to reinstate control over the oil flow in the well. The precise calculation of

the head or density of the drilling fluid required to bring the well under control is achieved through the simple hydrostatic relations.

$$H = \frac{P_R}{\rho_D g} \quad (1) \qquad \rho_D = \frac{P_R}{gH} \quad (2)$$

The two primary methods for injecting the drilling fluid into the well bore are known as recirculation and bull heading [2]. Recirculation requires there to be a connection made with the well's annulus, the space between the concrete casing of the well bore and the metal production tubing. It is then possible to pump the drilling fluid down the annulus and through a mechanically operated valve near the bottom of the bore hole. By injecting the heavier fluid near the bottom of the well it is possible to circulate out the formation fluid and replace it with the drilling fluid [2]. While this method is the most effective it is usually employed during planned kills rather than in emergency situations where the drilling rig becomes detached or cut off from the submerged well head. The faster method of drilling fluid injection is known as bull heading, and is the process of directly pumping drilling fluid into the well bore. By pumping the drilling fluids directly into the bore it is possible to force the formation fluids back into the oil reservoir while simultaneously increasing the hydrostatic head above the formation [2].

In the event that the well has been too badly damaged to be restored to production, these injection methods are then coupled with the injection liquid cement into the well bore in order to make a solid plug capable of sealing off the flow of the well completely. Once the cement solidifies it bonds to the steel production casing. The length of this plug is dependent on the bond stress and well diameter as follows.

$$F_T = (P_R - \rho_D g(H - h)) * A_r \quad (3)$$

$$L_C = \frac{F_T}{\pi d_W \tau} \quad (4)$$

The inherent problem with these strategies is they require complete control of the well flow in order to seal off the well entirely [2]. However, in uncontrolled well situations this control is not always possible due to the damage to the well tubing or casement. In these situations it is often difficult to regain

control over the well and prevent oil from leaking into the surrounding ocean as was seen in the recent BP Gulf incident. It would be useful to have the ability to temporarily alleviate the flow to allow for the positioning of equipment to enact one of the conventional top kill methods described above. The development of such a tool was the motivation for this thesis.

1.2   Adhesion and Cohesion Theory

In order to study the stresses associated with the adhesive bond strength of a material it is necessary to discuss adhesion and cohesion theory. This theory describes the two modes of bonding present in all adhesives that determine the adhesive's bonding effectiveness [3].

Adhesion characterizes the force between a substrate material and an adhesive that resists the separation of the two materials.
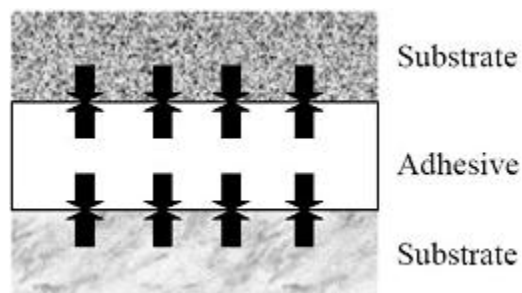
Figure 1.1: Adhesive forces are defined as the attractive forces between dissimilar surfaces [3].

This resistive force is the result of three different types of bonding, dispersive adhesion, mechanical adhesion, and effective adhesion [3]. Dispersive adhesion describes the intermolecular attraction between two contacting surfaces which is sometimes referred to as the macroscopic London-Van der Waal's Force. The London-Van der Waal attraction between two macroscopic surfaces is a function of surface geometries and their separation [4]. In order to determine the adhesion force associated with this type of adhesion it is first necessary to solve for the potential energy between the surfaces in proximity. As the potential energy is a geometric function it has been determined for a number of geometric configurations in **Appendix A**. The most common form of this equation is for plate geometries as shown in Figure 1.2 [4].
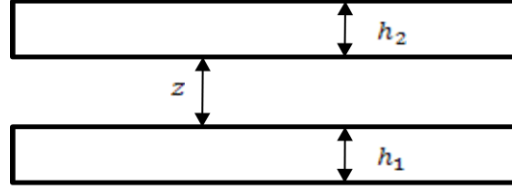
Figure 1.2: The parallel plate configuration for the determination of the Van der Waals forces [4].

Equation 5 can be used to relate the potential energy per unit surface area between the two parallel plates with thicknesses h_1 and h_2 at a separation distance z.

$$\frac{V_d}{A_S} = -\frac{A}{12\pi}\left(\frac{1}{z^2} + \frac{1}{(z+h_1+h_2)^2} - \frac{1}{(z+h_1)^2} - \frac{1}{(z+h_2)^2}\right) \quad (5)$$

A limiting case of particular interest in wetting studies occurs when $h_1 \rightarrow \infty$ then Equation 5 becomes

$$\frac{V_d}{A_S} = -\frac{A}{12\pi}\left(\frac{1}{z^2} - \frac{1}{(z+h_2)^2}\right) \quad (6)$$

By taking the inverse gradient of the potential function it is then possible to determine attractive force between two surfaces as follows.

$$F_d = -\nabla V_d = -\frac{dV_d}{dz} = -A_S\frac{A}{12\pi}\left(-\frac{2}{z^3} - \frac{3}{(z+h_1+h_2)^3} + \frac{3}{(z+h_2)^3} + \frac{3}{(z+h_2)^3}\right) \quad (7)$$

$$F_d = -\nabla V_d = -\frac{dV_d}{dz} = -A_S\frac{A}{12\pi}\left(-\frac{2}{z^3} - \frac{3}{(z+h_2)^3}\right); \quad when\ h_1 \rightarrow \infty \quad (8)$$

While these forces are important when dealing with the initial wetting of the surfaces they are weak in comparison to the forces associated with mechanical adhesion.

Mechanical adhesion results from the flow of adhesives into the microstructure of the surface of a substrate [5]. When the adhesive cures, or hardens in the pores and void spaces of the substrate it forms a mechanical bond to the surface that is capable of resisting imposed stresses. This is the most common form of adhesive bonding and it accounts for the majority of the adhesive bond strength. The third mode of bonding is known as effective bonding and is an optimized combination of both dispersive and mechanical bonds, to further increase the strength of the adhesion forces between the adhesive and the substrate [3].

While adhesion is the study of the attraction between adhesives and different substrate materials, cohesion is the study of the internal attraction between the molecules of the adhesive that holds the mass together.
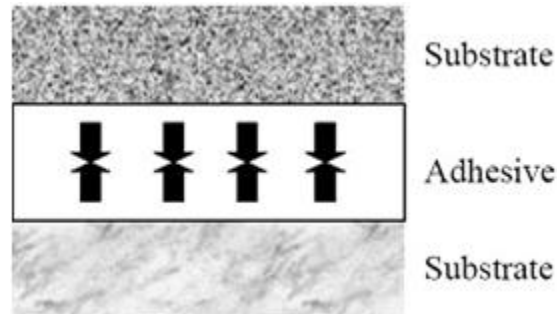
Figure 1.3: Cohesion is defined as the internal attractive force between the molecules of a material.

Cohesion is an intrinsic property that is dependent on the shape and structure of the adhesive's molecules which causes an irregular distribution of the electrons due to the molecules proximity to each other. The electrical attraction caused by this irregular distribution makes it possible for the material to maintain its macroscopic structure. The electrostatic force between molecules can be described by Coulomb's Law that models the interaction forces of a group of discrete charges. In the case of cohesion, the force is attractive rather than repulsive and can be described for a test molecule of charge q as a function of its proximity to the surrounding molecules within the structure of the adhesive.

The determination of the adhesive and cohesive strength is necessary to determine the likely mode of failure of an adhesive material when it is subjected to external stresses. While the theoretical approximations described can sometimes accurately predict the mode of failure in adhesives, experimental testing is usually necessary to confirm these theoretical models. By experimentally determining the maximum shear or tensile strength of the adhesive in question and observing the mode of failure it is possible to gain useful metrics for the comparison of different adhesives for particular applications.

1.3 Adhesive Strength Testing Methods

With the advent of new adhesive products in the past century the adhesive industry has established a number of standardized testing methods for the characterization of adhesive bond strength.

Since adhesive bonding is now used in a wide range of applications that are susceptible to both shear and tensile stresses it has been necessary to develop application specific metrics to allow for the comparison of different adhesive products. The existing test methods are directed towards determining one or more of the following properties of adhesives to provide a basis of comparison.[5]

- Adhesive Elastic Tensile or Compressive Modulus
- Effective Adhesive Transverse Modulus
- Characteristic Adhesive Shear Strength
- Characteristic Adhesive Tensile or Compressive Strength
- Adhesive and Adherend Elastic/Plastic Shear Stress and Strain
- Adherend Tensile or Compressive Modulus
- Adherend's Poisson Ratio
- Characteristic Adherend Through-Thickness Tensile Strength
- Adhesive Layer Thickness
- Thickness of Adherend
- Joint Efficiency

Adhesive testing methods can be divided between those methods used to determine physical properties, to aide in the selection of an adhesive, and those used to determine the quality of adhesively bonded structures, to aide in the design of adhesive joints [6]. Unfortunately these standardized methods and there metrics are limited by the dependence of adhesion on the test specimen geometry [6]. Due to the complex state of stress that exists in the adhering layer for different geometries the majority of these tests are incapable of providing reliable universal engineering parameters for use independent of the application [6]. However, using the metrics available from the existing test procedures it is still possible to gain an understanding of the adhesive bond strength on a geometry and material specific basis.

When dealing with applications for adhesives the properties of interest are the characteristic adhesive shear or tensile strength. The American Society Testing Materials Standards (ASTM) has developed a number of testing methods and standards for different geometries to allow for the comparison of adhesives on an application specific basis. The experimental methods associated with these standards are known as shear-tension, tensile, and peel testing.

1.4.1Shear-Tension Testing Methods

One method of determining the characteristic adhesive shear strength of adhesives is known as the shear tension method or in-situ testing [8]. Using a table of ASTM standard test methods in

Appendix B it is possible to find a number of different geometries that are designed to produce a state of shear loading while minimizing other loads either in the bulk of the adhesive or within the adhesive layer depending on expected failure mode, either cohesive or adhesive failure [7]. In these tests the characteristic adhesive shear strength is a simple function of the adhered surface area and the experimentally determined average maximum load force as seen in Equation 10.

$$\tau = \frac{F_L}{A} \qquad (10)$$

The most widely used test geometries associated with the shear-tension method are known as lap joints. Lap joints can take on a number of different geometries in order to determine the adhesives bond strength for different joint constructions. The most common lap joint configurations can be seen in Figure 1.4 [8].
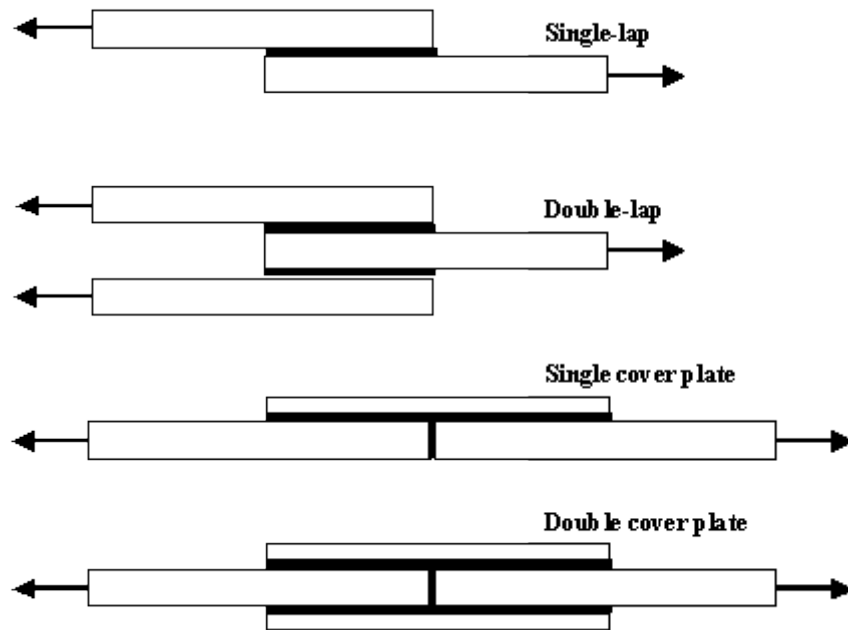
Figure 1.4: Various lap joint test configurations [8].

ASTM lap joint shear tests also make use of a standard adhered surface area of with a width of 25mm and length of 100mm, with a variable adhesive thickness depending on whether the test concerns adhesive of cohesive failure [7]. In a single lap joint construct the adhesive is applied to one of the test plates that make up the joint. The second plate is then laid to overlap the adhesive coated section of the

other plate. The length and width of this overlapped section can be varied in order to determine which dimension will have a critical limit, where an increase in the variable will have a negative effect of the maximum load the sample can withstand before failure. Other than being a function of length and width of the adhered area the critical shear load is also highly dependent on the substrate material as shown in Figure 1.5.
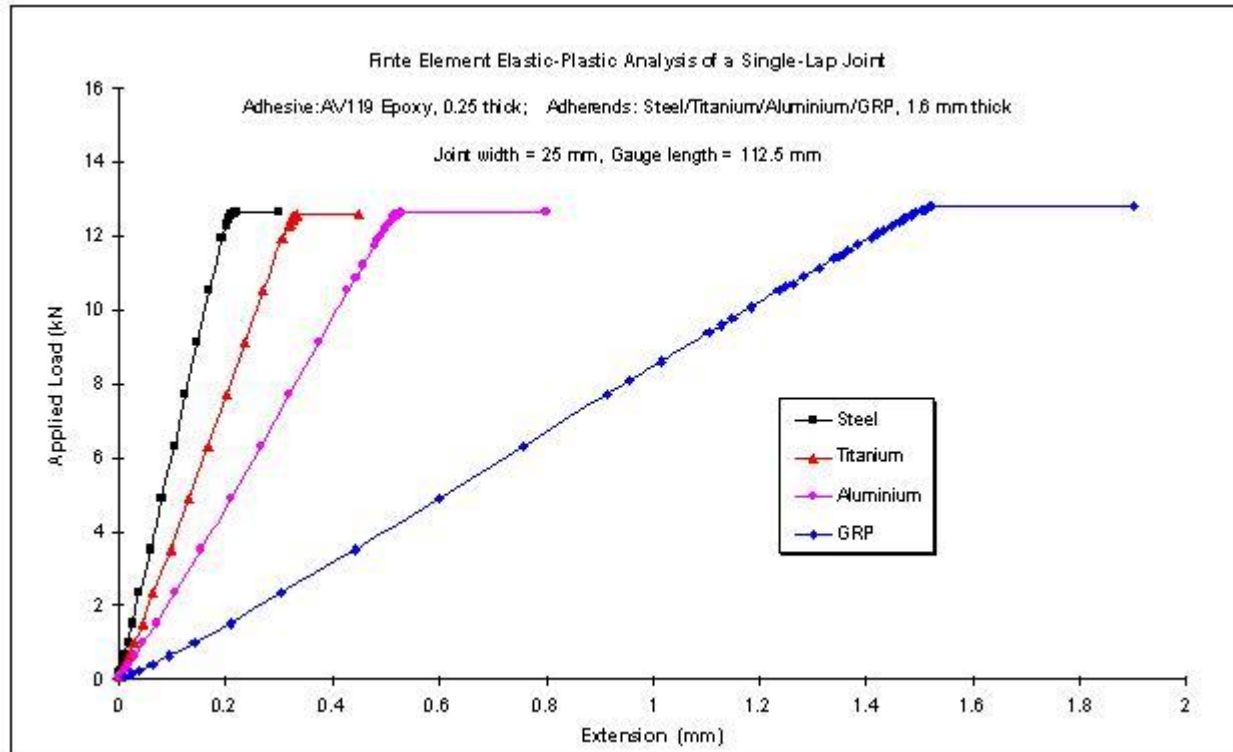
Figure 1.5: Typical single-lap joint load-displacement response for different substrate materials [8].

In this case the shear force is given as a function of strain. Using the relation above it is then possible to determine the maximum shear stress as a function of strain which will allow for the determination of the characteristic shear strength of the adhesive.   The failure of moss adhesives is caused by the complex stress profile across the bondline, or length of the adhesive, shown in Figure 1.6.
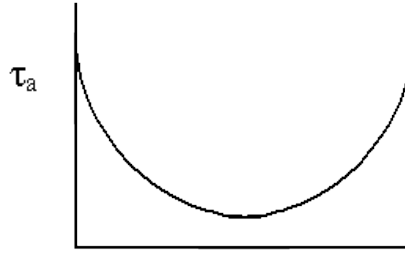
Figure1.6: The non uniform shear stress (τ_a) distribution results in the creation of stress concentration near the ends of the adhesive.[8]

Failure is due to the creation of stress concentrations at the either end of the adhered area. By increasing the overlap length of the lap joint it is possible to decrease the average shear stress and increase the load capacity of the material; however, this will also cause an increase in the stress concentration at the ends of the adhered area. For this reason there exists an optimum ratio of length over adhesive thickness (L/t) after which increasing the length of the adhered area will no longer effectively reduce the shear stress concentration and peel stresses, described in Section 1.3.3, exhibited on the adhered area.[8] For most design applications the optimal ratio of around thirty and is called the ineffective length [9].

It is also possible to increase the load capacity of the adhesive in question by increasing the width of the adhered area. The width of this area is directly proportional to the failure load of the adhesive. Essentially if the width of an adhesive were doubled the failure load capacity of the adhesive would also double. This relationship makes it clear that in order to impact the load capacity of the adhesive without impacting the shear stress distribution the width rather than the length of the adhered area should be increased [9]. While there has been no substantial testing of cylindrical adhesives it is possible that increasing the diameter of the adhesive will have the same impact on the material's adhesive.

1.4.2 Tensile Butt Joint Testing Method

The tensile testing method is used to directly measure the characteristic tensile strength of adhesives [10]. This is desirable because it is a measure of the response of the adhesive under the most severe loading conditions possible since adhesives are weakest when subjected to tensile stresses. Like

the shear-tension method the tensile testing method has a number of different test fixtures that can be used to test the characteristic tensile strength of specific adhesives [10]. Of the many different ASTM fixtures developed to determine this strength the butt joint method is one of the most reliable. The experimental cross section and test fixture are shown in Figure 1.7.
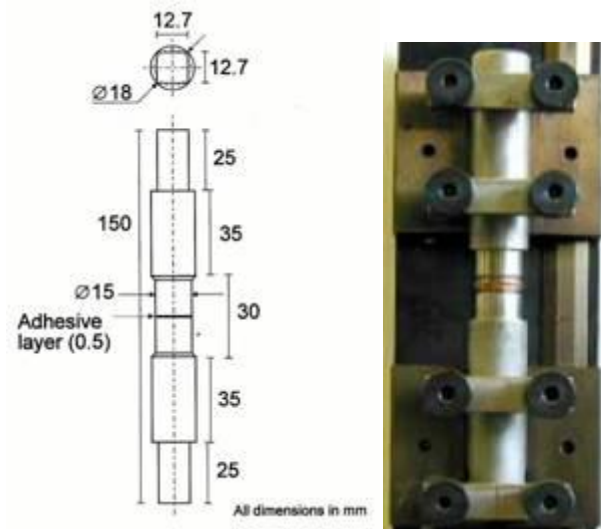
Figure 1.7: Experimental configuration for the tensile butt joint test method.[10]

By applying a tensile load on one side of the test fixture it is possible to determine the maximum load an adhesive can withstand before failure. It is also possible to use this method to determine many other useful engineering properties such as the modulus of rigidity, modulus of elasticity, and Poisson's Ratio. As in any other experimental technique the butt joint method is susceptible to error due to the misalignment of the two cylindrical sections of the device. In the case of any misalignment, it is possible to expose the adhesive specimens to shear stresses that can seriously impact the measure tensile strength of the adhesive. To limit this interference the apparatus has a number of features built into it that allows for the automatic realignment of the two halves of the test fixture.

While the butt joint is a common test method used in industry it is not very useful in determining the adhesive bond strengths of complex geometry. As this thesis is concerned with the experimentation of the adhesive bond strength of a cylindrical surface this method will not be utilized.

1.4.3 Tensile Peel Test Method

Another method of adhesive tensile testing is referred to as a "peel" test. In a peel test there is an indirect measurement of the tensile force necessary to remove a thin adhesive layer from a substrate [12]. In these tests force is not applied directly to the adhered joint as in the butt joint tests. Rather the force is applied along a moment arm as shown in Figure 1.8.
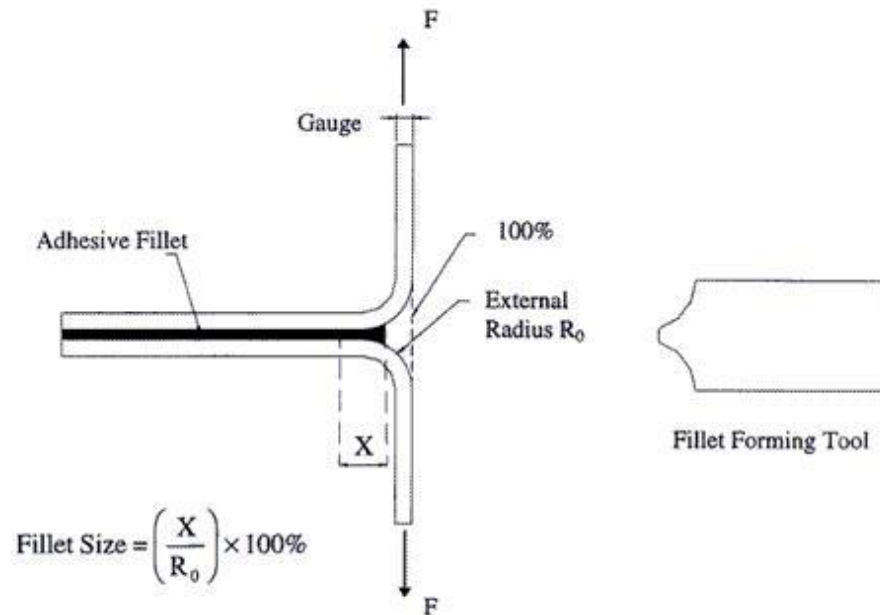
Figure 1.8: Experimental configuration for the tensile peel test method [12].

The most common type of peel test is the T-Peel test which is widely used to determine the "peel resistance" and peel strength of an adhesive. Peel resistance is measured by the angle to which the two plates can be separated to prior to the failure of the adhesive. This is a qualitative measure that is widely used in the adhesives industry due to its reliability for the comparison of flexible adhesives [11]. A more quantitative measure known as the peel strength is defined as the average peeling load per unit width of the bondline. A common force response for a peel adhesion test can be seen in Figure 1.9.
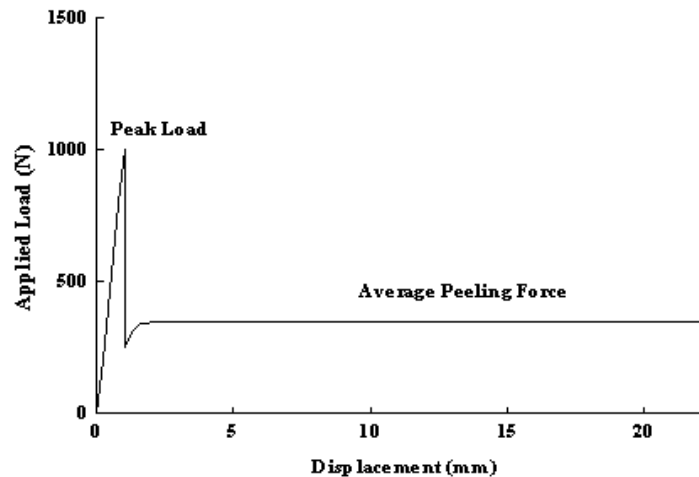
Figure1.9: Typical force-displacement curve for a T-Peel test where displacement is the measure of the distance between the plates [12].

From these test it is possible to find both the peak peel load as well as determine the average peeling force of the adhesive. It has also been shown that the peel strength is a strong function of adhesive thickness and adhesive stiffness. Extensive testing has shown that when the adhesive thickness increases the peel resistance will increase while the average peel strength will tend to decrease. Conversely, if the adhesives stiffness is increased, the peel strength will increase, but the peel resistance will decrease [12]. Understanding the effects of adhesive stiffness on the peel strength of an adhesive material is important to this thesis as the material being experimented on forms a rigid gel. Fortunately, as the peel test results confirm, the stiffness of the "oilygel" material will limit the peel experienced near the stress concentrations described in Section 1.4.1.

1.5 "Oilygel" Fabrication

Over the past year research was conducted by Justin Griffin, in cooperation with Aspen Aerogels, on "oilygel" in order to optimize a recipe and mixture procedure for the formation of uniform volumes of the gel. "Oilygel" is comprised of 3-aminopropyltriethoxysilan (APTES), Silbond H5 (H5), 3-isocyanatopropyltriethoxysilan (ICTES), and a liquid hydrocarbon, in this case 10W-30 Motor Oil. In order to fabricate a uniform "oilygel" plug it was necessary to control the mixing process to assure the complete distribution of the chemical constituents in the mixture. However, in order to allow the

formation of the internal cohesive structure of the "oilygel" the mixing procedure must be stopped prior to the beginning of the phase change of the liquid mixture. Through trial and error it was possible to determine the optimal mixing time for the "oilygel" samples to allow for the distribution of the chemical constituents without negatively impacting the formation of the internal cohesive structure. The optimized recipe and mixing procedure used for the reliable formation of "oilygel" samples is shown below.

"Oilygel" Recipe

1) 5 ml Silbond H5

2) 5 ml 3-Aminopropyltriethoxysilan (APTES)

3) 5 ml 3-Isocyanatopropyltriethoxysilan (ICTES)

4) 2.1 g of 10W-30 Motor Oil

Mixing Procedure

1) Begin by preparing the required volumes of the separate constituents in a fume hood.

2) Prepare a glass beaker to form the gel in.

3) Add the 5ml of Silbond H5 with the 2.1g of 10W-30 Oil to the test beaker inside of a fume hood to provide adequate ventilation.

4) Add the magnetic stirring rod to the test section and place the test section on the magnetic stirrer.

5) Activate the stirrer at 1000rpm.

6) Add 5 ml of APTES to the mixture.

7) Add 5ml of ICTES to the mixture wait 30 seconds and turn off the mixer.

8) Wait 3 minutes to provide adequate time for the internal structure of the gel to form.

9) Unseal the end of the test section to perform mechanical testing.

2. Experimental Method

2.1 "Oilygel" Gelation Methods

Building on the past "oilygel" research a method of gelation was developed that allowed for the creation of a cylindrical "oilygel" plug in a steel test section to be used on the experimental apparatus. It was found that the "oilygel" required vigorous mixing to assure the complete diffusion of the chemical components in order to create an "oilygel" plug of uniform density. Due to the need for this mixing during the initial stage of the gelation process two methods were devised to allow for the implantation of the gel in the test section prior to the phase shift of the mixture. The test section used in this experiment was a tubular piece of low carbon steel with an internal diameter of 25.4 mm and exterior diameter of 63.5 mm. A picture of this test section can be seen in Figure 2.1.

The first method allowed for the gelation of the sample in the test section. By mixing the chemical constituents in the test section it is was possible to assure the formation of adhesive bonds between the gel and the substrate walls.
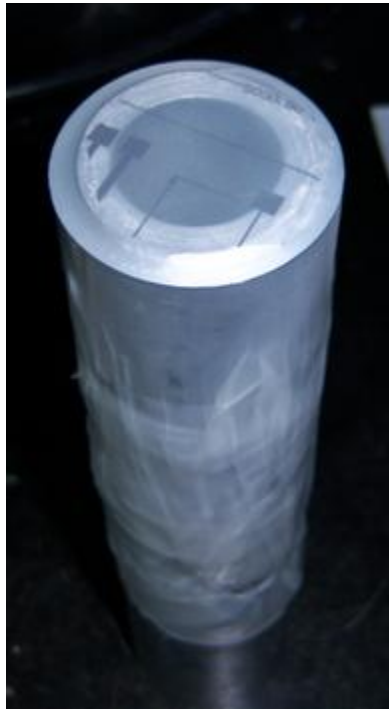
Figure 2.1: The test section is sealed on one side using a piece of laminate plastic to cover the cross section of the tube while it is sealed using Para-Film.

For this method one end of the test section was sealed as shown in Figure 2.1 and the constituents of the gel were added and mixed according to the following process.

Gelation Method #1:

1) Add the 5ml of Silbond H5 with the 2.1g of 10W-30 Oil to the test section inside of a fume hood to provide adequate ventilation.

2) Add the magnetic stirring rod at and place the test section on the magnetic stirrer.

3) Activate the stirrer at 1000rpm.

4) Add 5 ml of APTES to the mixture.

5) Add 5ml of ICTES to the mixture wait 30 seconds and turn off the mixer.

6) Wait 3 minutes before performing mechanical testing.

7) The magnetic stirrer rod will be integrated into the internal structure of the adhesive.

The modified methods for the formation of samples of different volumes can be found in Appendix C. The second gelation method increased the time required for the phase transition of the mixture by decreasing the percent by volume of the APTES and ICTES monomers. This allowed for the constituents to be mixed in satellite glasswear before being poured into the test section and allowed to gel. For this method the timing of the transfer of the components from the mixing vessel to the test section was critical to maintaining their uniform distribution and allow for the creation of adhesive bonds. This method is shown below and the methods for samples of different volumes can be found in Appendix C.

Gelation Method #2:

1) Mix the 2.1g of oil and the 5ml of APTES, which is a very miscible system, in the mixing vessel in a fume hood to provide adequate ventilation during the mixing process.

2) Add magnetic stirring rod to vessel and place it on the magnetic stirrer.

3) Add the 5ml of ICTES to the mixture and stir at 600 rpm for 30 sec.

4) Add the 20 ml Silbond H5.

5) Allow the constituents to mix for 45 seconds after the addition of the Silbond H5.

6) Transfer the mixture to the test section within 10 seconds of the end of the mixing stage.

7) During the transfer the magnetic forces between the stirring rod and the steel test section should allow it to cling to the top of the test section allowing for its removal from the mixture. If the test section was non magnetic then a pair of tweezers was used to remove the stirring rod before the transfer to the test section.

8) Gel should require about 70 seconds to solidify after the addition of Silbond H5, which should allow for the transfer from glassware to the test section.

9) Wait 4 minutes before performing mechanical tests.

2.2 Design of Experimental Apparatus

Due to the lack of an adhesion testing method that can output reliable engineering parameters for universal application it is necessary to develop a testing method to conduct in-situ, situational specific, testing of the "oilygel". With this in mind a rig was designed to determine the adhesive bond strength as a function of adhered surface area of different adhesive "plugs" in a cylindrical geometry. In order to measure the force required to break the adhesive bonds formed by the "oilygel", this apparatus was designed to exert a compressive load on the cross section of the specimen. In order to provide accurate measurements of the load being exerted on the test specimen, the apparatus required a load cell capable of relaying data to a data acquisition program. To fulfill both of these requirements the testing rig was designed to be installed on a table top Instron testing fixture and make use of Bluehill Lite Software. The load was then exerted on the specimen through the use of a compressive piston that was installed on the cross head of the Instron as shown in Figure 2.2.

Figure 2.2: The load piston can be attached to the load cell though the use of 6mm Clovis pin connection.

In addition to the load piston there are four other major components that make up the apparatus. They are the test section, test section housing, alignment plate, and anti-deflection plate. The design specifications of these components can be found in Appendix D. The test section was used to hold the sample during testing and its design is discussed in Section 2.2.1. The test section housing was designed to allow the priming of the piston, which is discussed in Section 2.2.2, and maintain the concentricity of the test section with the load piston to prevent any interference between the two pieces during testing. The other two components comprise the base of the apparatus. They were designed to be directly

installed on the Instron as seen in Figure 2.3. This allows for the test section and test housing to be

mounted concentrically beneath the load piston to minimize the chance of interference between the test

section or the housing and the piston during its movements, as shown in Figure 2.3.
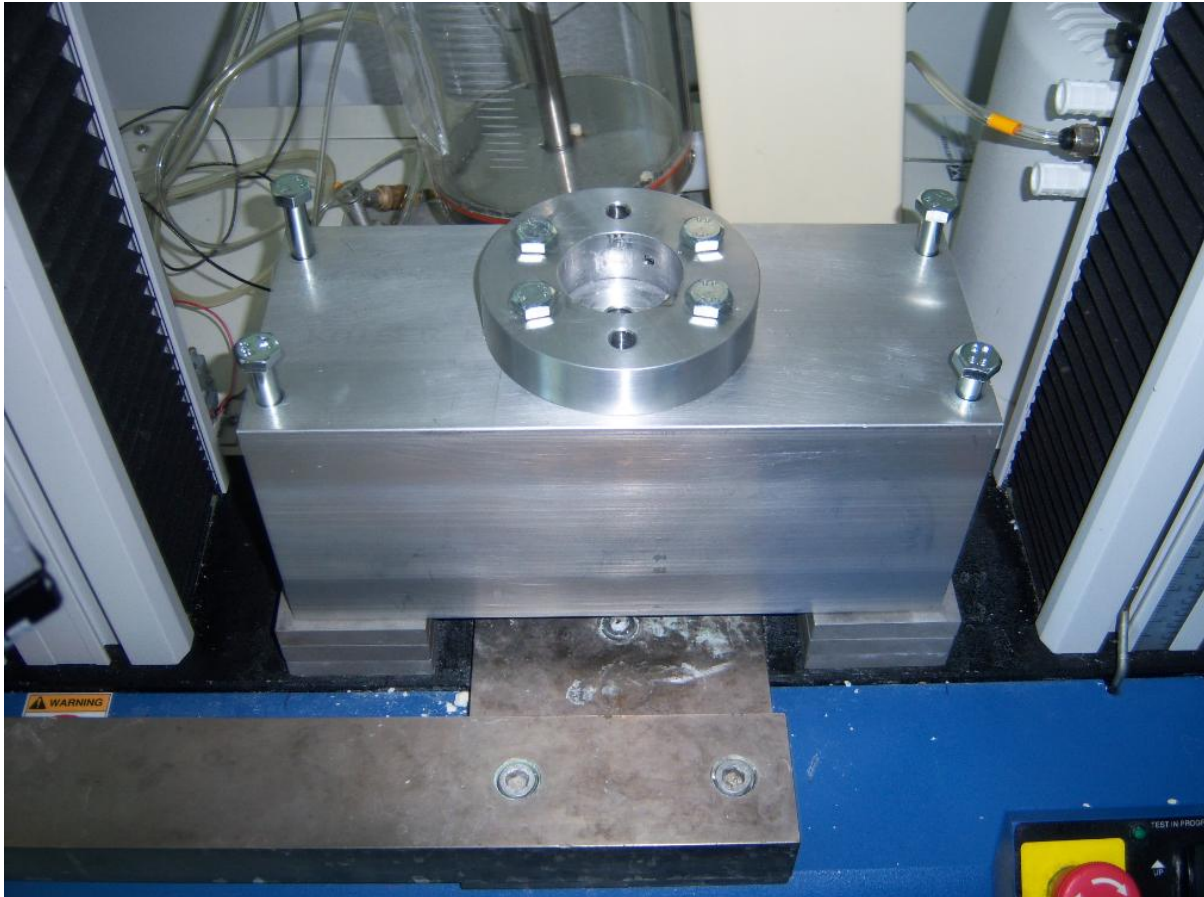
Figure 2.3: The alignment plate and anti deflection plate were design to be installed directly on the base of the Instron which ensures the concentricity of the test section and housing between tests.

The anti deflection plate shown in Figure 2.3 was designed to prevent any appreciable deflection in the

system that could skew the data being collected. In order to experiment with different loading

mechanisms, the testing rig was designed to allow for the application of force directly to the sample using

the load piston or through use an incompressible liquid interface.

2.2.1 Shear Test Section Design

Since the adhered surface area of the test specimen was a function of two variables, the

specimen's length and diameter, it was necessary to conduct tests where only one of these was varied.

This was done to determine the nature of the dependence of "oilygel's" bond strength on a particular

parameter.   Fortunately, for the proposed application it is not possible to vary the diameter of the gel;

therefore, the diameter of the test section was held constant. This apparatus was therefore designed to

allow for the variation of the specimen's length while maintaining a uniform cross section. The test

section was designed to be removed from the apparatus to allow for the gelation of the "oilygel" as

described in Section 1.1. As adhesive strength can also depend on the substrate material and its

roughness a number of different test sections were created to allow for testing with various materials and

roughness conditions.

2.2.2 Force Transmission Medium

In order to achieve a uniform loading condition on the cross section of the test specimen it was

convenient to make use of incompressible liquid 10W-30 motor oil medium to apply the load rather than

having the load piston come into direct contact with the sample. This method of force transmission

required the apparatus to be completely sealed to assure that the measured force was exclusively applied

to the specimen's cross section. The rig was outfitted with three of o rings designed to withstand the

pressure associated with driving the fluid without leakage as shown in Figures 2.4 and 2.5**.**

Figure 2.4: The static o-ring was designed to prevent the permeation of the force transmission medium into the annulus between the test section and test housing.

Figure 2.5: The dynamic o-ring installed on the load piston set was designed to prevent the force transmission fluid from displacing upward during testing.

A static o-ring is located in a gland between the removable test section and the test section housing to prevent leakage into the annulus between the test section and the housing. The dynamic o-ring set was installed on the load piston and was designed to prevent leakage while the piston was moved downward. In order to assure the seal of the piston o rings it was necessary to prime them in the upper section of the housing. To avoid pre loading the specimen through the compression of air trapped between the piston and the liquid interface a high pressure elbow valve was used to bleed off this pressure while the piston was lowered into place. Once the piston was primed this valve was also used to assure that only the liquid occupied the space between the piston and test specimen as shown in Figure 2.6.
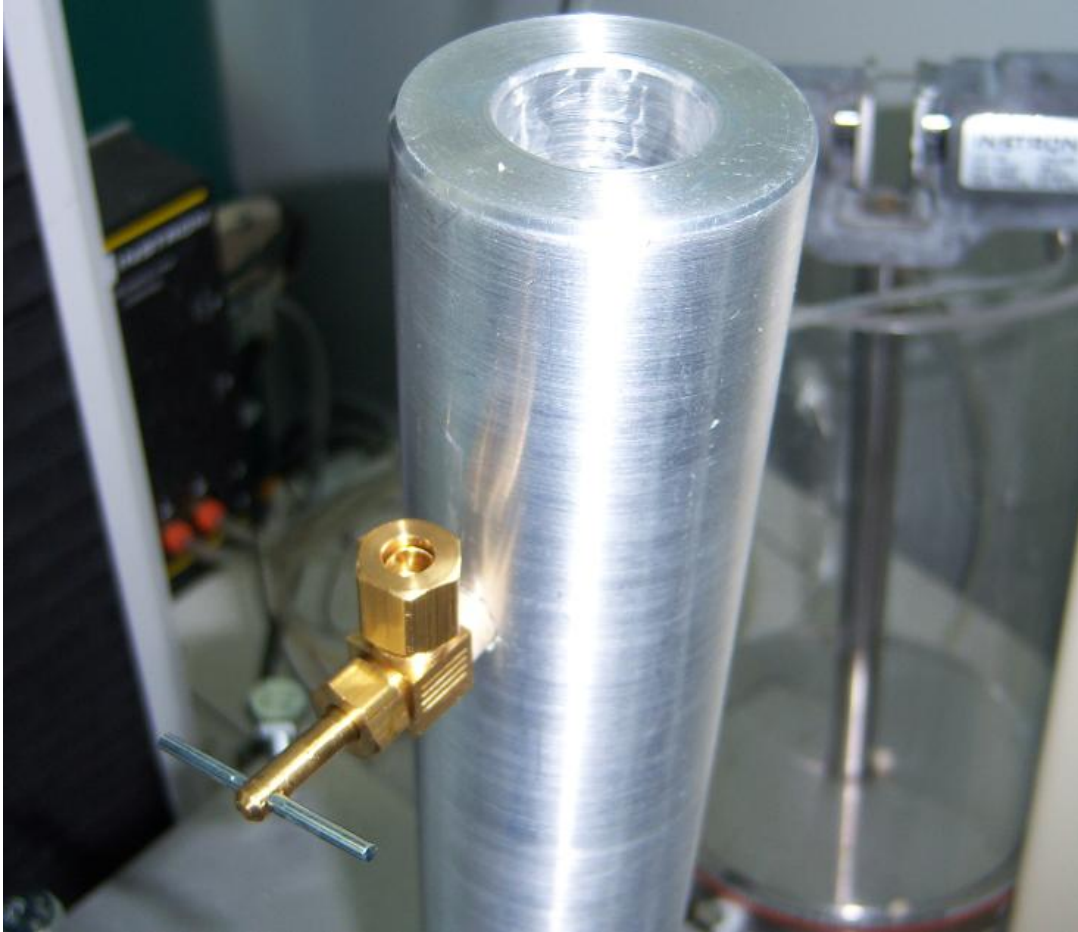
Figure 2.6: The elbow valve is used to purge the air from the system by displacing it with oil.

2.3   Construction of the Experimental Apparatus

The construction of the experimental apparatus occurred from December 2010 to January 2011 in preparation for testing during the spring of 2011. The majority of the components were manufactured in house at the Bray Laboratory while a few were contracted to the Colby Street Machine Shop. Once the components where machined they were installed on the Instron Test Fixture to assure that the parts had been properly manufactured and would not interfere with each other during experimentation

2.4   Data Acquisition & Control System

The data acquisition system used for this experiment was comprised of an Instron load cell and the Bluehill Lite Software interface.   The load cell used in our experiments was an Instron 2530 Series Low-profile Static Load Cell rated for the accurate measurement of a load range of ±100 N. This load

cell is shown in Figure 2.7 and is designed to be interchangeable with other load cells depending on the

load range of interest. The complete specifications of these load cells can be found in Appendix E.
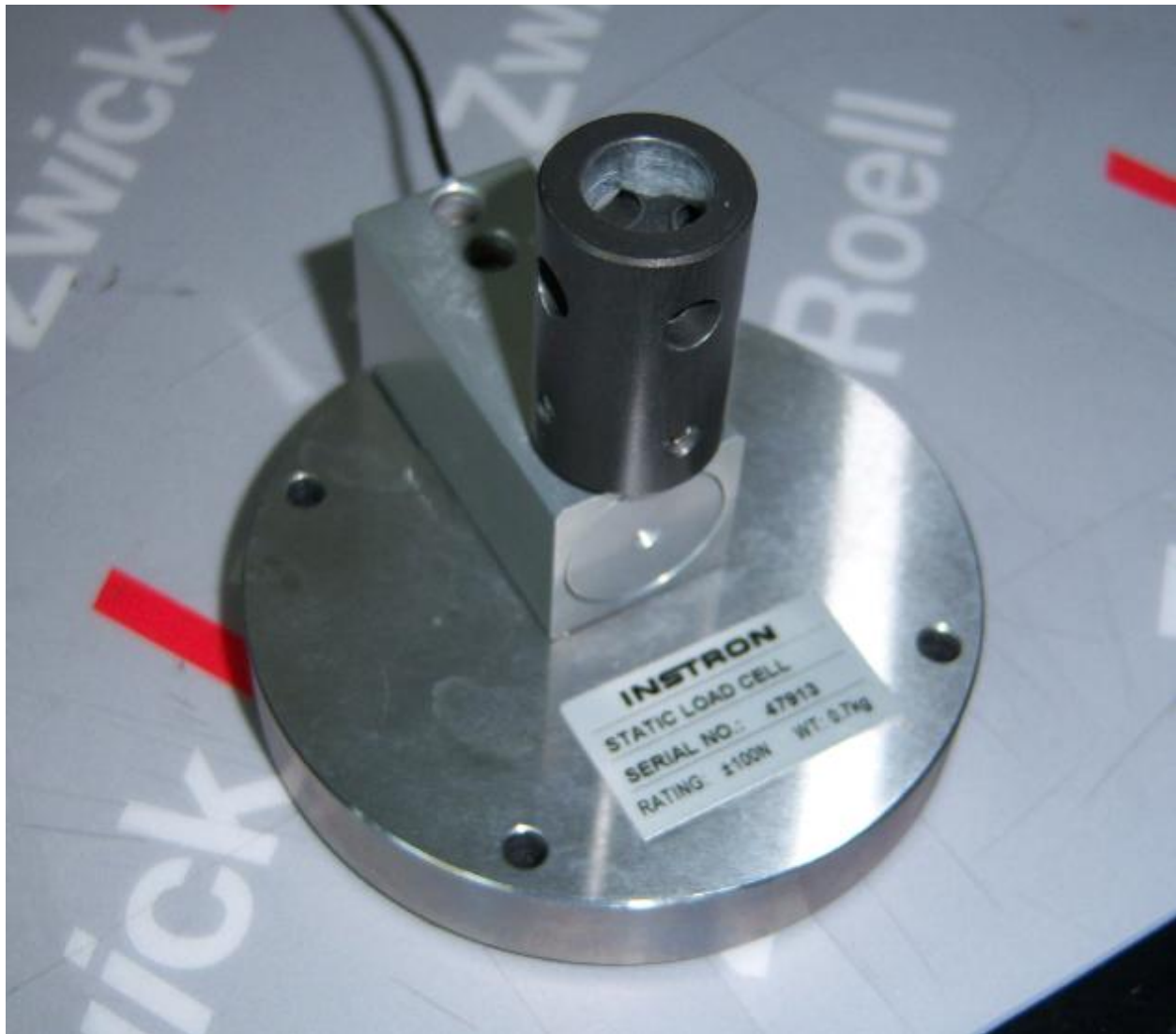
Figure 2.7: A 2530 Series Low-profile Static Load Cell was used for the accurate collection of data within a range ±100 N.
Data was collected using the Instron Test Fixture's link to a nearby computer terminal capable of

supporting the Bluehill Lite Software. The Bluehill Software allowed for the control of the load being

exerted on the test specimens through the control of the Instron's crosshead. This software allows for the

creation of test methods, which are essentially executable programs that automatically control the

movements of the Instron during testing. The software interface also allowed for the user to balance the

load being measured by the load cell and zero the position of the crosshead to allow for the creation of

data points as shown in Figure 2.8.
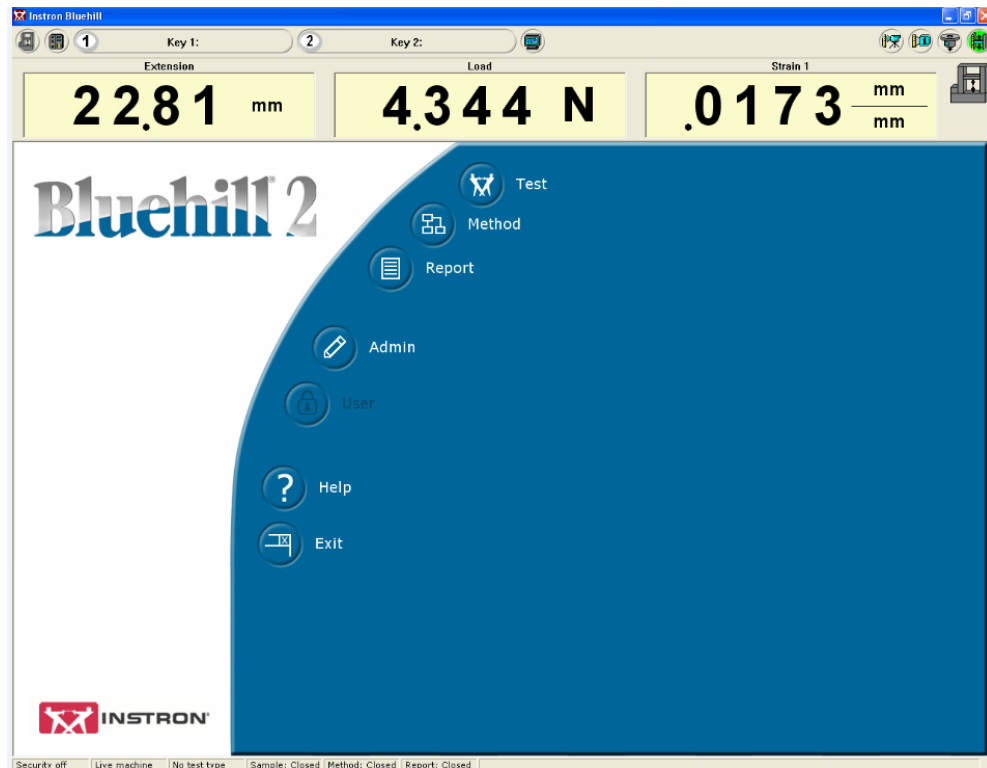
Figure 2.8: Bluehill Lite Software control panel.

This interface also provided control over what data was being collected and which data set was being

monitored during testing. An example of the testing interface used during this experiment is shown in

Figure 2.9.
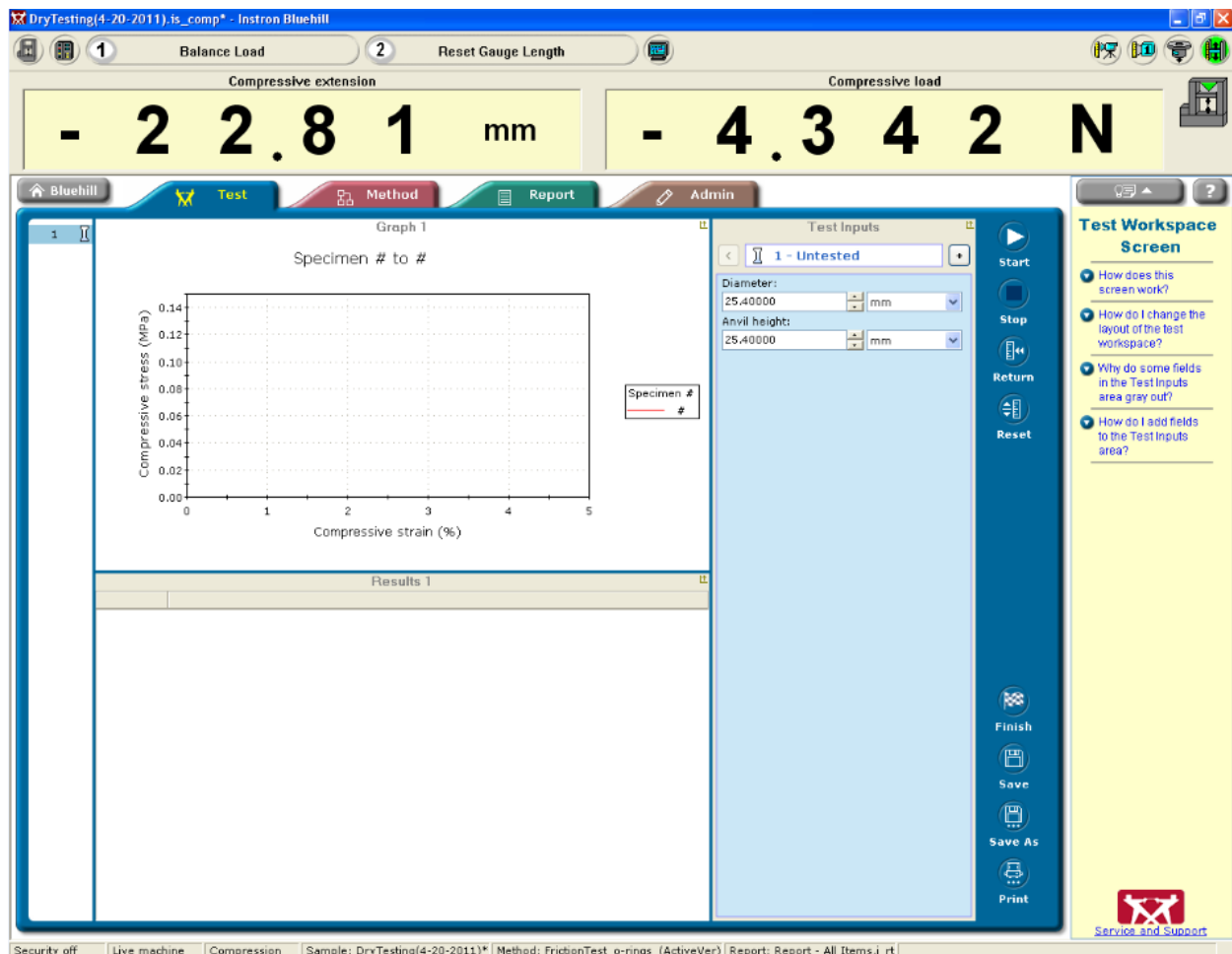
Figure 2.9: Screenshot of the shear compression test method used in this experiment.

2.5 Instron Testing Methods and Apparatus Calibration

A basic adhesive shear strength testing procedure was established for use of the experimental apparatus while installed on the Instron 3366 Test Fixture. This procedure was developed in order to maintain the repeatability of the test between experiments. This procedure is comprised of three different sections apparatus preparation, friction calibration, and compressive load testing.

2.5.1 Instron and Apparatus Preparation

Prior to beginning the adhesive strength test using the experimental apparatus and the Instron it was necessary to initialize the Instron Testing Frame and the Bluehill Lite Software to gain control of the cross head and move it out of the way to install the apparatus. Once the cross head was moved and the base of the Instron was cleared it was then possible to install the apparatus on the Instron.

In order to reduce the error associated with conducting multiple tests using the same apparatus it was necessary to prepare the apparatus before each battery of adhesion tests. This preparation involved cleaning the test section, test housing, and load piston to remove any residue from the testing surfaces using metallic test tube brushes, steel wool scrubbers, and industrial surfactants. This was done before and after each adhesion test making it possible to replicate the test conditions for each consecutive test. In addition, by standardizing the installation of the testing apparatus on the Instron Testing Fixture it was possible to preserve the concentricity of the test section, test housing, and load piston between tests to ensure the repeatability of the adhesion tests. The components of the apparatus were specially manufactured to be installed directly on the Instron's base, in the case of the anti deflection and alignment place, and the Instron's cross head, in the case of the load piston. This was done to maintain the concentricity of these parts by screwing in the bolts through the base as shown in Figure 2.10, and then mounting the test housing, test section, and load piston.
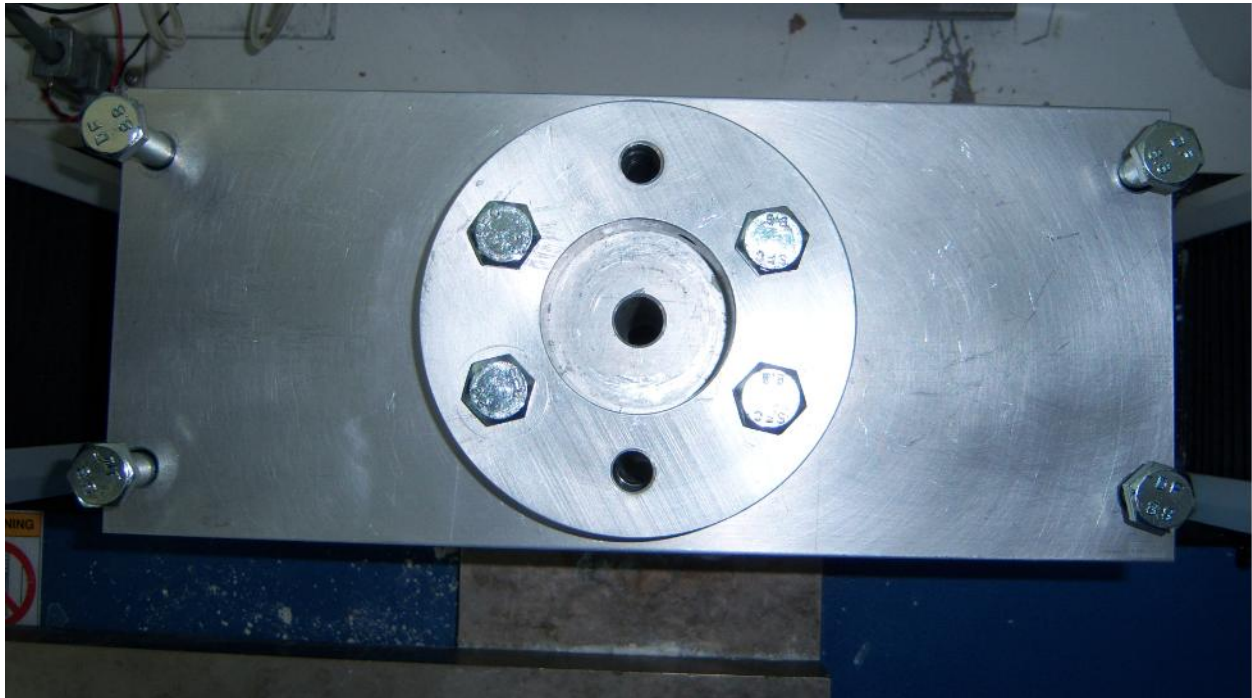
Figure 2.10: Top view of the base mount used to center the test section and housing beneath the load piston.

In order to make small adjustments to the position of the housing for a better alignment with the load piston it was possible to adjust the set screw in the alignment plate shown in Figure 2.3. Once the

components had been installed the load cell was reset to account for the weight of the load piston on the load cell.

2.5.2 Compressive Load Testing & Friction Calibration

Once the apparatus had been properly installed of the Instron Test Fixture it was then necessary to launch the compressive loading method that was developed for our test through the Bluehill Lite Software. The test method for this experiment was modeled after simple compression test where a load is exerted over a cross section by moving the cross head of the Instron down at a constant rate. When the test method designed for this experiment was initiated on the Bluehill interface the load piston displaced downward a distance of 25.4mm at a rate of 5 mm/s to allow for the accurate measure of the maximum load supported by the test specimen before failure. The main data set of interest for this testing method was the force response of the specimen at each position along its path of motion.

Before activating the program it was necessary to decide whether the test would make use of a transmission medium or direct contact to exert a load on the test specimen. In the case the of the direct contact method the load piston was lowered to approximately 2 mm above the test specimen where the gauge length was reset. When using a transmission medium the load piston was lowered 66.45 mm from a datum at the top of the test housing. A new datum was recorded at this position and the piston was then removed from the test housing where the load cell was reset before being returned to the defined datum point to begin testing. The predefined program was then initiated using the Bluehill interface. Once the test ran to completion the load piston was raised out of the test housing and removed from the load cell. The housing was then uninstalled and the test section removed. Using the load piston, the test specimen was then pushed through the remaining length of the test section. In order to preserve the sample for further examination it was quickly removed from the atmosphere and stored in an air tight container due to the tendency of the samples to degrade when exposed to the air for extended periods of time.

When performing consecutive testing the test housing, test section, and load piston were cleaned as mentioned above. The test section was then taken to the hood to gel another specimen for

testing. Once the specimen was prepared the components were then reinstalled on the Instron test fixture for further testing.

Unfortunately, due to the manufacturing methods used to create the different components of the experimental apparatus there was always the possibility of friction due to, proximity of the load piston and the test housing and test section. In order to properly account for this error it is necessary to run a series of five friction tests without a specimen gelled within the test section to determine the friction experienced by the load piston when it is moved downward during the compressive load tests. Using the average frictional force response at each point as determined by these tests it was then possible to account for its effect on the data recorded during the adhesive strength tests.

2.5.3 Transmission Medium

When conducting tests using a force transmission medium rather than through direct contact it was also necessary to install the dynamic o rings on the load piston. For this case it was still necessary to conduct the frictional calibration described in Section 2.5.2. Additionally it was necessary to assure that no air became trapped between the load piston and the test specimen as described in Section 2.2.3.

3. Results

3.1 Data

Data was collected from the Instron load cell using the Bluehill Lite Software and the method described in Section 2.5. Once the data was collected using the data logging software it was then exported and processed in Microsoft Excel. Using Excel it was then possible to calculate the dependence of force on the length of the sample as well as determine the average shear stress over the area of the cylinder. For this round of testing the direct contact method of force application was used to exert a force on the test specimen. This method was chosen due to the unrepeatability associated with the force transmission tests for samples that were less than 60 mm in length.

3.2 Direct Contact Tests

Adhesive testing of the "oilygel" tested four different lengths to provide an adequate range of data to extract trends for the force and shear stress responses of the "oilygel" as a function of length. Each test group was composed of samples within a length range of ±5 mm of each other. The variation of length within each group was caused by the thermal expansion of the mixture due to the exothermic reaction of the constituents. These test specimens were prepared using *Gelation Method 2* as described in Section 2.1 in a test low carbon steel tubular test section an inner diameter of 25.4 mm. For each length range a minimum of three "oilygel" specimens were gelled and tested. Some groups have fewer samples than others depending on the agreement of the force responses of the samples.

3.3 Relevant Calculations

The two parameters of interest in this experiment were the force response and the shear stress on the adhered area of the specimens. In the case of the force response it was necessary to adjust for the frictional forces on the piston during its motion from the datum. This was accomplished by averaging the collected frictional force data at each point along the piston's path and then subtracting these values from the measured force response of the "oilygel" specimens along the same path. Using the adjusted force measurements it was possible to find the average shear stress on the adhered surface. The average shear stress was determined using the simple correlation show in by Equation 4.1.

$$\tau = \frac{F_A}{(\pi * D * L)} \quad (11)$$

Using these two parameters it was possible to see the effect increasing the specimen's length had on load capacity of the "oilygel". Using the critical load and shear stress data from all of the samples, trends for the behavior of these parameters as functions of length were developed.

3.3.1 Adjustment for Friction

Prior to testing the first group, the Bluehill Software was used to test the frictional response of the movement of the load piston from the selected datum to the final displacement of 25.4 mm. The adjustment was the average of all fifteen frictional response tests as shown in Figure 3.1.

Average Friction Force Response vs. Displacement
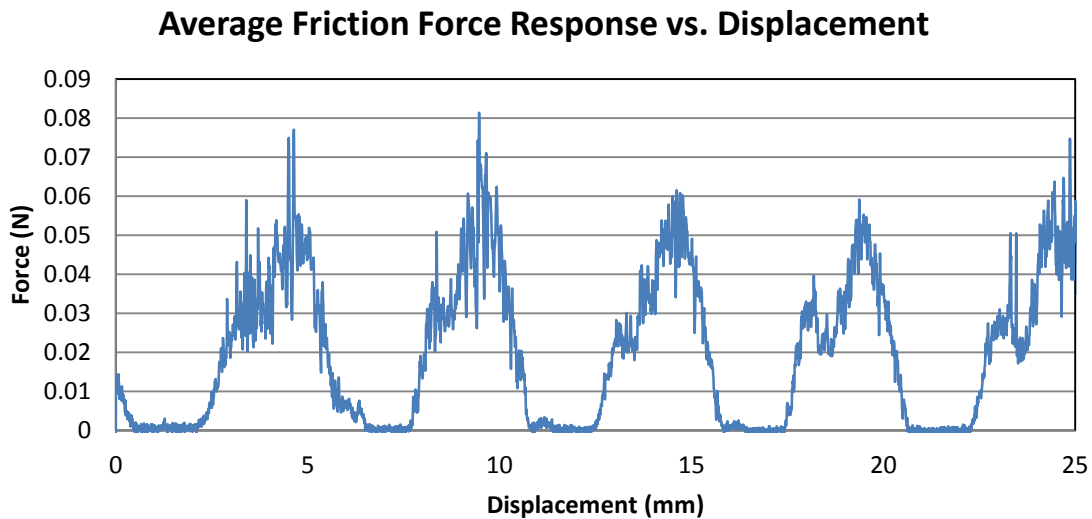
Figure 3.1: Average Friction Force Response during the motion of the Load Piston took on a sinusoidal shape due to oscillations caused by the actuation of the Instron's cross head. These oscillations caused the piston to come into contact with the side walls of the test section housing with a relatively constant frequency as shown.

Fortunately the friction had a relatively small in impact on the force measurements for out tests as the maximum friction force was .079N. Regardless this average friction force trend was then used to adjust the force measurements of the different specimens. The adjusted force plot for test group one that was comprised of samples with a mean length of 38.14mm is shown in Figure 3.2.

Adjusted Force vs. Displacement (L$_{mean}$ = 38.14 mm)
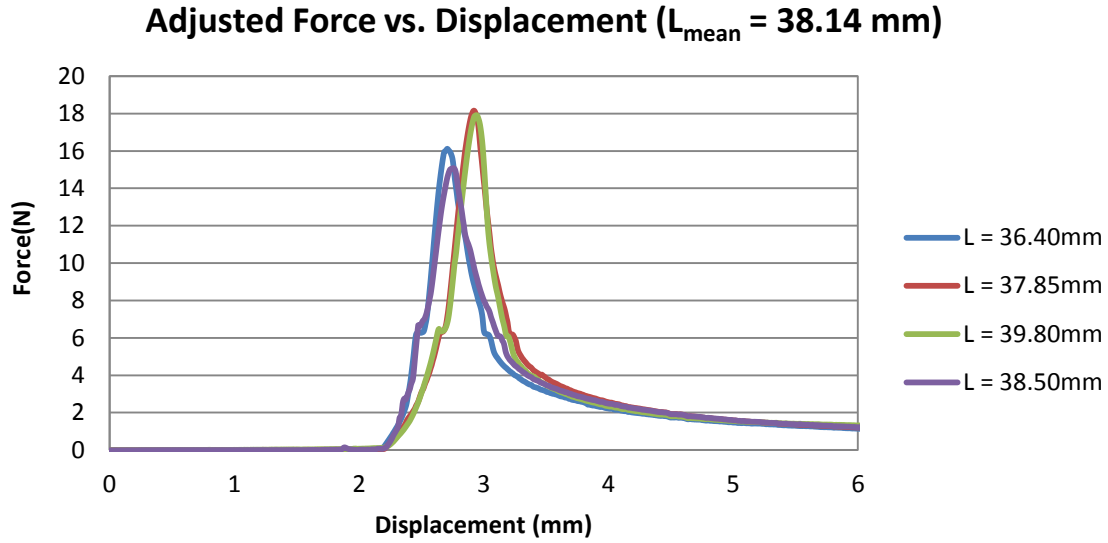
Figure 3.2: Adjusted Force Response of "oilygel" samples with a mean length of 38.14 mm.
The adjusted force response for test group two that was comprised of samples with a mean

length of 56.72 mm is shown in Figure 3.3.

Adjusted Force vs. Displacement (L$_{mean}$=56.72 mm)
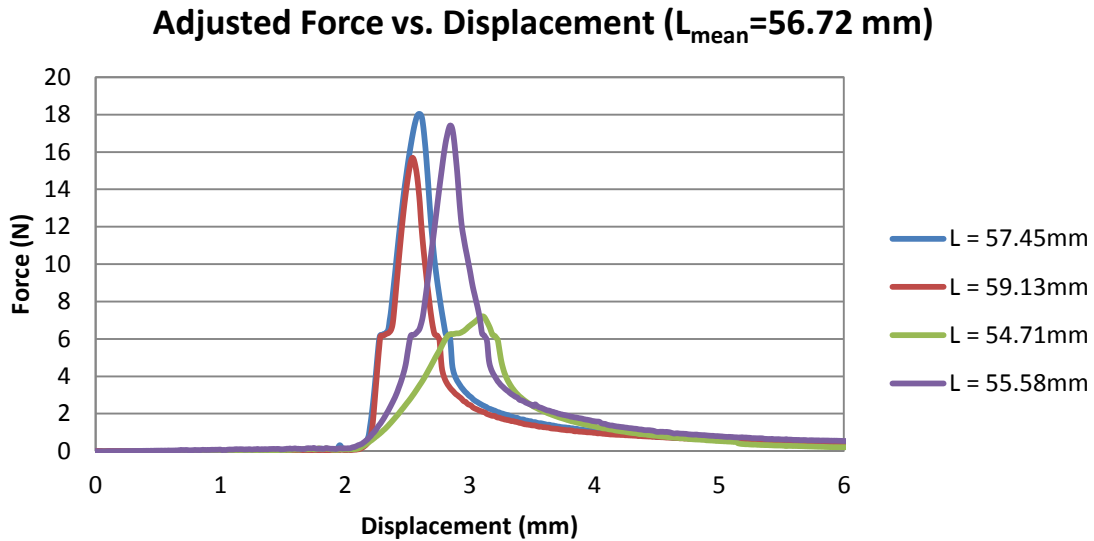
Figure 3.3: Adjusted Force Response of "oilygel" samples with a mean length of 56.72 mm.
The adjusted force plot for test group three that was comprised of samples with a mean length

of 81.26 mm is shown in Figure 3.4.

Adjusted Force vs. Displacement (L$_{mean}$=81.26 mm)
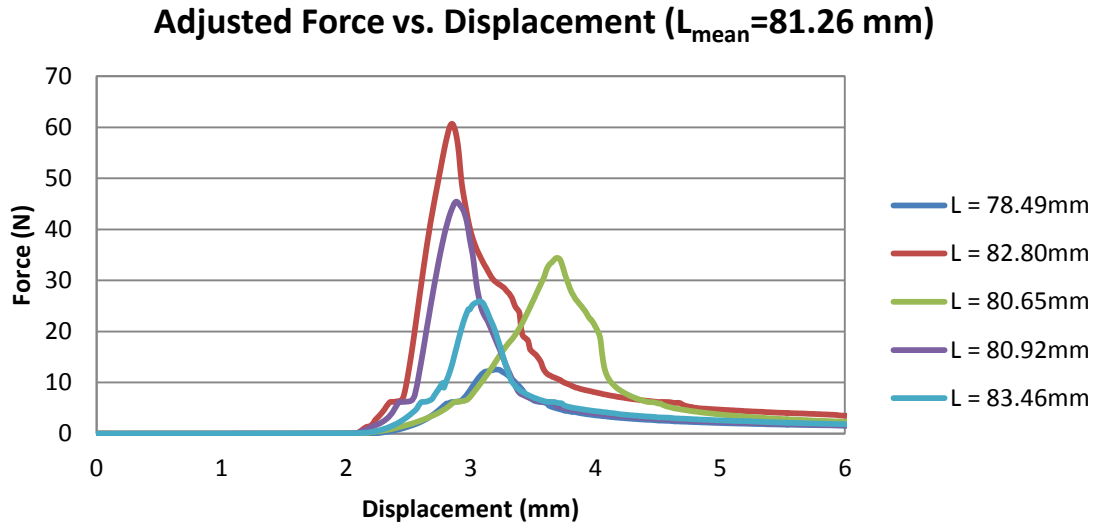
Figure 3.4: Adjusted Force Response of "oilygel" samples with a mean length of 81.26 mm.

Group three was tested most extensively due to the relative lack of repeatability in the test data. Unlike the other three test groups the results from this group were scattered providing no reliable information on the response of this length range of "oilygel".

The adjusted force plot for test group four that was comprised of samples with a mean of length 105.10 mm is shown in Figure 3.5.

Adjusted Force vs. Displacement (L$_{mean}$=105.10 mm)
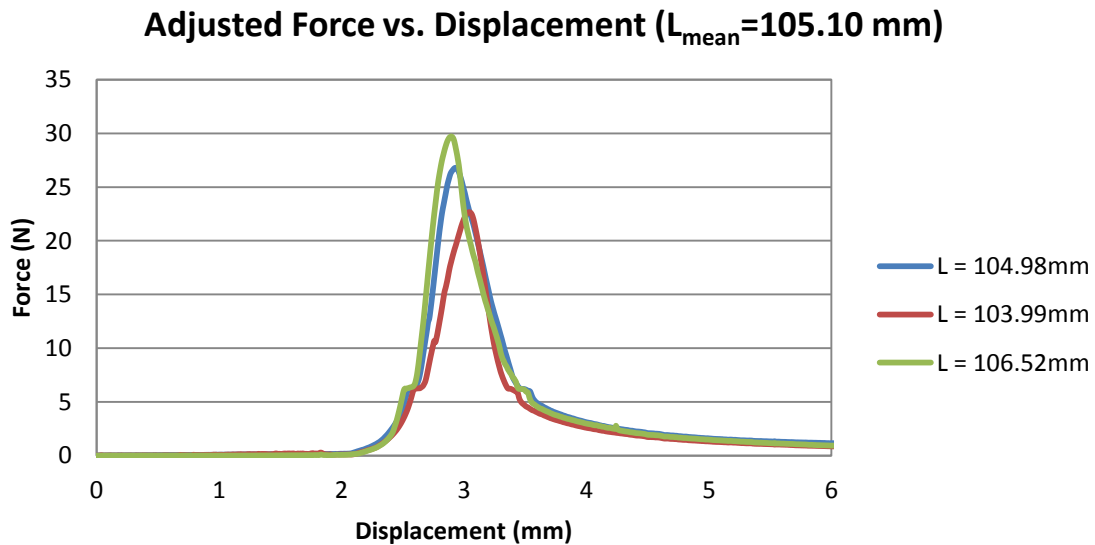
Figure 3.5: Adjusted Force Response of "oilygel" samples with a mean length of 105.10 mm.

3.3.2 Shear Stress Determination and Specimen Correlations

After performing the frictional adjustments on the force responses of each specimen the shear stress was determined according to the Equation 11. The shear stress of test group one that was comprised of samples with a mean length of 38.14 mm is shown in Figure 3.6.
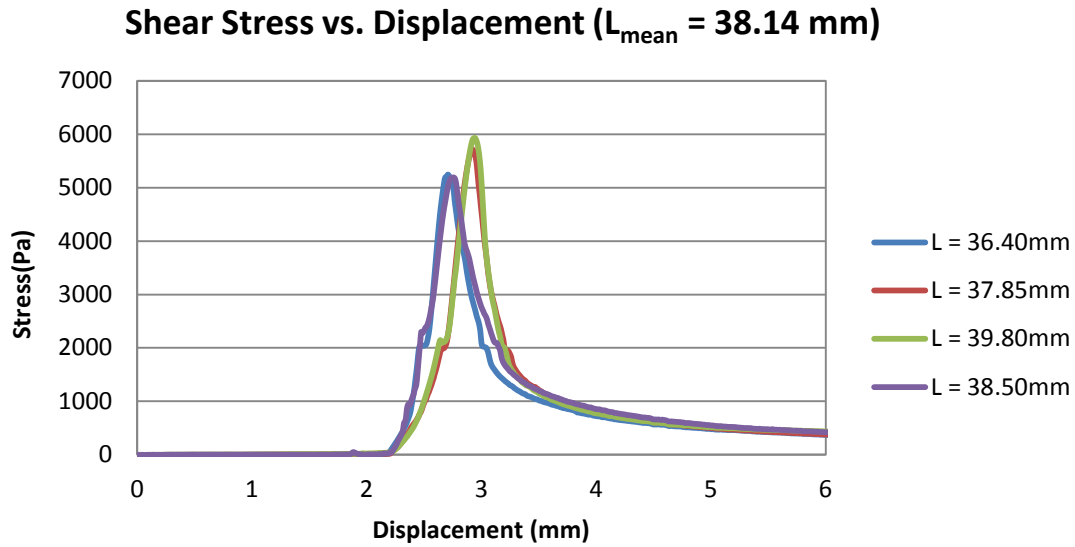
Figure 3.6: Shear Stress on the adhered surface of the "oilygel" samples with a mean length of 38.14 mm.

The shear stress of test group two that was comprised of samples with a mean length of 56.72 mm is shown in Figure 3.7.
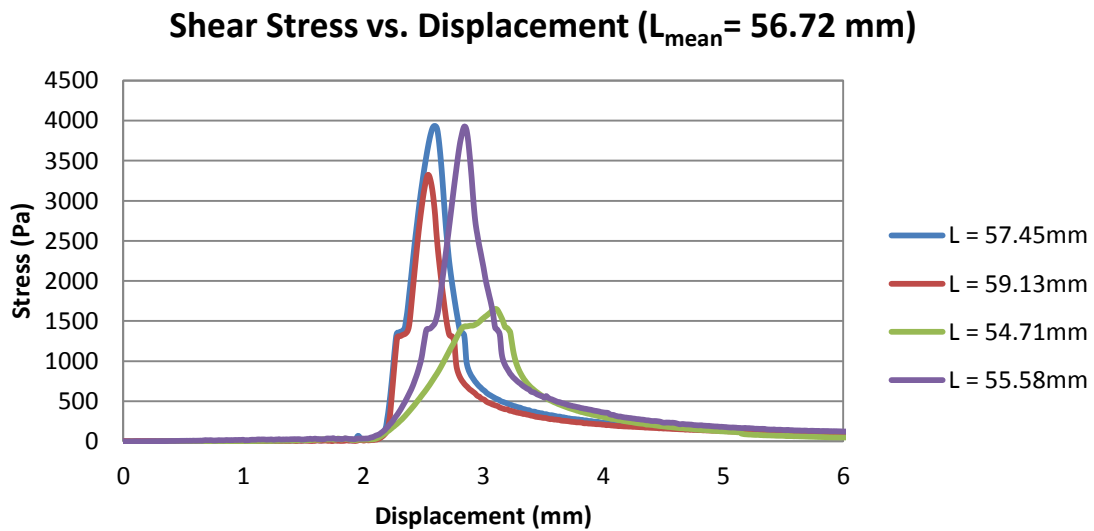
Figure 3.7: Shear Stress on the adhered surface of "oilygel" samples with a mean length of 56.72mm.

The shear stress of test group three that was comprised of samples with a mean length of 81.264 mm is shown in Figure 3.8.

Shear Stress vs. Displacement (L$_{mean}$=81.26 mm)
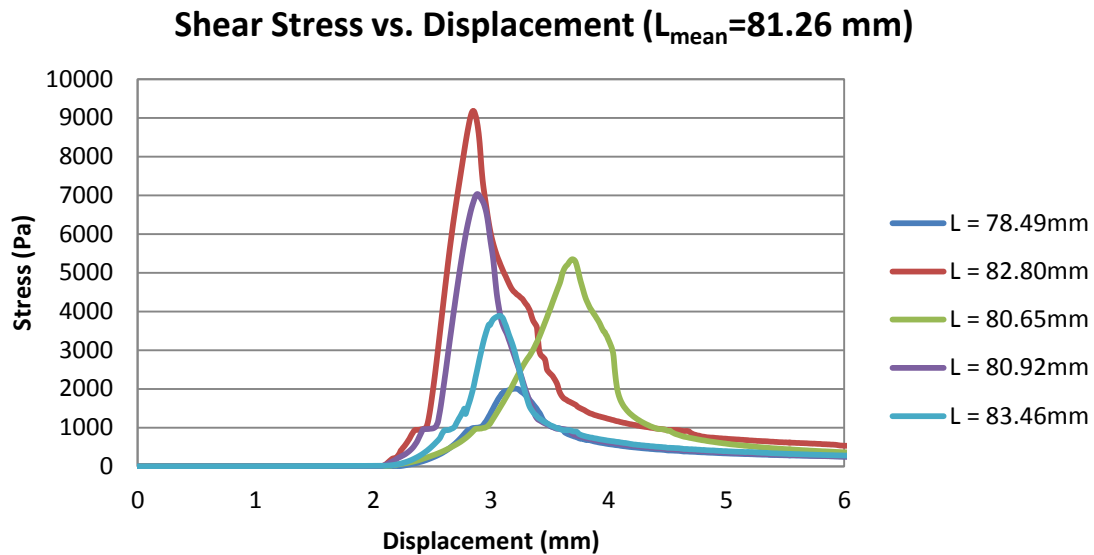
Figure 3.8: Shear Stress on the adhered surface of "oilygel" samples with a mean length of 81.26 mm.
The shear stress of test group one that was comprised of samples with a mean length of 105.10 mm is shown in Figure 3.9.

Shear Stress vs. Displacement (L$_{mean}$=105.10 mm)
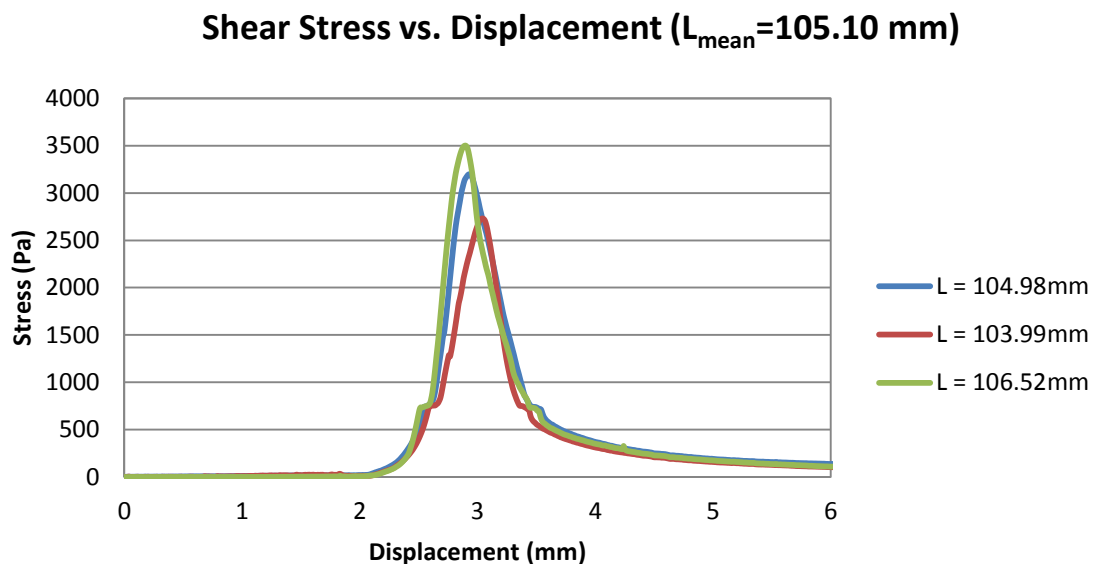
Figure 3.9: Shear Stress on the adhered surface of "oilygel" samples with a mean length of 105.10 mm.
Using the adjusted critical force and shear stress values for the samples is was possible to develop trends for these parameters as a function of length. The critical force trend is shown in Figure 3.10 while the critical shear stress trend is shown in Figure 3.11.

Critical Force vs Specimen Length

y = 339.85x
R² = 0.2196
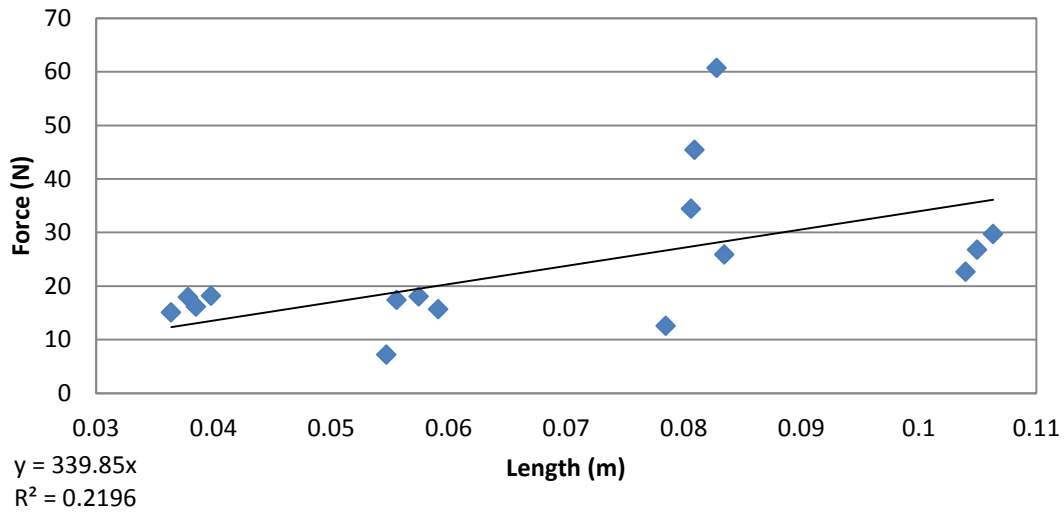
Figure 3.10: Plot of the adjusted maximum critical force values of the samples versus their individual lengths. The trend developed for this data set has a low agreement of $R^2 = 0.2196$.

Critical Shear Stress vs. Specimen Length

y = -14558x + 5489.8
R² = 0.0343
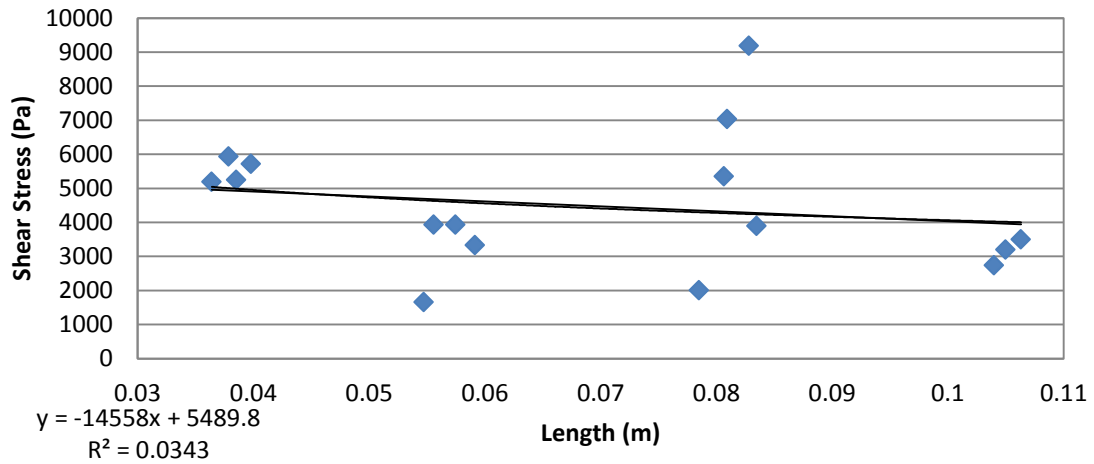
Figure 3.11: Plot of the calculated maximum shears stress values of the samples versus their individual lengths.

4.   Discussions

4.1   Testing Method Adjustments

Throughout the testing process the methods of gelation and compressive testing were streamlined to provide more repeatable results.   These changes can be used to explain some of the seemingly random error in our results.

4.1.1 Gelation Method

A more efficient means of mixing and transferring the chemicals greatly reduced the creation of non uniform samples that were causing a large variation in the force measured by the Instron load cell during testing. Unfortunately this process had a learning curve as seen in the results of group three in Section 3. During testing the method of transferring and mixing the chemicals constituents of the "oilygel" changed from being poured from a number of satellite glassware pieces into a main mixing vessel, to being transferred using a pipette dropper with an accuracy of ±0.005 ml to reduce chemical loses. This adjustment allowed for the fabrication of "oilygel" samples of uniform density for experimentation. This adjustment can be clearly seen in the data from the increase in the precision of critical force measurements for the other three test groups showing that we needed to retest the third group to acquire accurate data for that sample length. The wide variation in the third group's data revealed how even minor mistakes made during the mixing procedure can cause large variations in the expected load response of the sample. In the context of the proposed application this could be extremely problematic as the turbulent flow seen in oil wells could easily cause the incomplete gelation of the "oilygel" or all together prevent the formation of the gel.

4.1.2 Limitations on the Force Transmission Medium

During preliminary experimentation with the Instron and the test apparatus there were a number of tests using the force transmission medium. Unfortunately these tests had very mixed results mostly due to permeation of the medium through the plug causing large variations in the load being measured by the Instron. After refining the gelation method as described in Section 4.1.1 it was possible to attain a test where the medium did not permeate through the gel, which suggests there is a direct

relation between the gelation processes and the porosity of the material. Unfortunately this test method also required there to be a preloading on the sample of around 23.79N caused by the hydrostatic pressure of the 10W-30 Motor Oil used for the transmission medium. This pre loading condition restricted the testing of samples of low lengths so ultimately it was not used during this round of testing.

4.2   Uncertainty in Results

The majority of the uncertainty of this experiment can be attributed to the gelation process itself. Even with the refinements described in Section 4.1.1 it isn't possible, with the current mixing and transfer method, to assure the uniform diffusion of the chemical constituents in the mixture. Since the formation of mechanical adhesive bonds, as described in Section 1.2, is directly related to the permeation of the liquid mixture into the pores and cracks of the substrate prior to the phase change. It is reasonable to see that the lack of gelation along the adhered surface would have a serious impact of the measured critical force of the specimen. Once again this can be most easily in the results of group three, as the percentage of adhered area, and therefore the critical force, was raised through the refinement of the chemical transfer and mixing process.

In addition to the error caused by the gelation process there was also error inherent with the different systems used for data collection and the preparation of the "oilygel" specimens. The main components used for data acquisition were the Instron load cell, Instron displacement measure, and a digital caliper. The Instron 2530 Series Low-profile Static Load Cell was capable of measuring the load to within ±0.0001 N and the Instron displacement measure was capable of determining the cross head position to within ±0.001m. The digital caliper used to measure the specimens after their removal from the test section had an accuracy of ±0.001mm. The pipette dropper used for chemical measurement and transfer had an accuracy of ±0.005 ml. Fortunately the accuracy of this equipment had little effect on the overall uncertainty of the experiment.

4.3   Theoretical Model

After reviewing the data from Section 3 it is possible to see that the force response of all of the samples fell off exponentially after the critical load was reached. This means that nearly all of the

measured adhesive bond strength can be attributed to the initial formation of bonds during the phase transition of the "oilygel" mixture. If this is the case then it is accurate to model the response of the "oilygel" using only the critical force as a function of length. This function was determined from the experimental data in Section 3.3. With the omission of the results of group three, for the reasons discussed in Sections 4.2, it was possible to increase the agreement of this trend with the remaining experimental data by nearly 30% as shown in Figure 4.1.

Critical Force vs Specimen Length with Group Three Ommited

y = 162.08x + 8.3779
R² = 0.5716
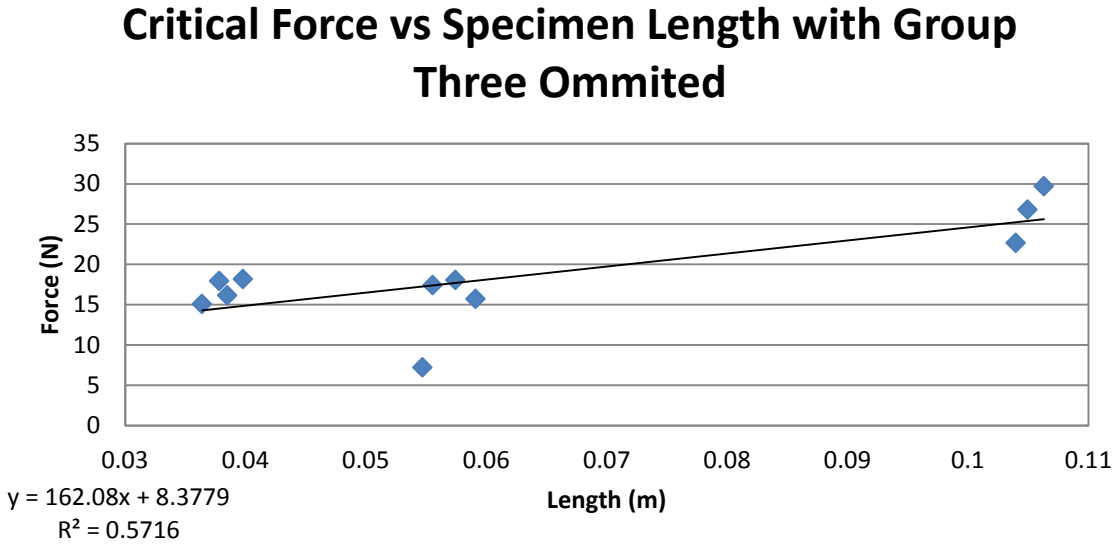
Figure 4.1: Plot of the adjusted maximum critical force values of the samples versus their individual lengths with group three omitted. The trend developed for this data set has an increased agreement of $R^2 = 0.5716$.

The trend lines equation can be rewritten in the form shown by Equation 12.

$$F(L) = 162.08 \left(\frac{N}{m}\right) * (L) + 8.3779N \quad (12)$$

This equation can then be modified to provide the average shear stress on the adhered section of the "oilygel" as shown in Equation 13.

$$\tau(L) = \frac{162.08\left(\frac{N}{m}\right)}{\pi * D} + \frac{8.3779N}{\pi * D * L} \quad (13)$$

Unfortunately as described in Section 1.3.3 the shear stress is a widely non-uniform distribution over length of the specimen. This decrease in average shear stress would suggest that the adhesive bonds became weaker with longer specimen lengths; however, this is not the case. This decrease in mean shear stress is balanced by an increase in the shear stress concentrations at either end of the sample. It is this

shear stress concentration that causes the failure of the adhesive bonds. So perhaps a more useful metric for this application can be expressed as the compressive stress that the "oilygel" plug can withstand as a function of length as shown in Equation 14.

$$P(L) = \frac{4 * \left(162.08 \left(\frac{N}{m}\right) * L\right)}{\pi * D^2} + \frac{4 * (8.3779N)}{\pi * D^2} \quad (14)$$

However, it is possible that the "oilygel" could be susceptible to the same ineffective length condition that was exhibited by adhesives in lap joint tests as discussed in Section 1.3.1. If this is the case it is likely that the function for the compressive stress shown in Equation 4.4 would change after a certain length. If the ineffective length ratio is the same for the "oilygel" as it was for other adhesives it is possible that the problem of diminishing returns for the compressive stress could begin as quickly as only thirty diameters of length. This is due to the reduction of the effectiveness of length to diffuse the peel stresses and critical shear concentration at the ends of the sample.

5.   Conclusion and Future Work

In order to access the viability of the "oilygel" product as a means of controlling and sealing renegade oil wells an experimental apparatus was developed to determine the load characteristics before failure as a function of the length of the "oilygel" in a cylindrical geometry. This apparatus was constructed to allow "oilygel" samples of varying length to be tested under uniform conditions in order to develop a reliable model for the response of the gel under compressive loads.

This apparatus was designed to exert a compressive load on the sample to determine the critical stress required to break the adhesive bonds that the gel sample formed with the cylindrical substrate material. It was assumed that the bulk of the "oilygel" sample was essentially rigid and therefore would only deform under shear.   For this reason the apparatus was designed to exert a purely shear load on the sample to determine the shear force required to deform and break the adhesive bonds.   This was accomplished by applying a uniform load across the entire cross section of the sample. Under these loading conditions the effects of peel and tension forces on these bonds could be minimized. In order to assure the even distribution of load stress on the test specimen, two mechanisms of loading were developed. The first of these methods involved the direct contact of a load piston with the top of the sample while the second method relied on the use of an incompressible medium to transfer the load to the sample. Using the data collected from these experiments it was then possible to develop a model for the load response of the "oilygel" as a function of length.

After the optimization of the experimental testing method a number of samples were successfully tested and it was possible develop an experimental trend for the critical load force and stress as a function of specimen length. Based on a 25.4 mm cross section and a typical formation pressure of 32.06 MPa this experiment showed that the "oilygel" plug would need to be 100.17 m in length. For a typical production casings are around 127 mm this length would need to be around 1604.4 m. However, adhesive strength had been shown to increase with the width of the

adhered area so this length could be appreciably shorter. Regardless this length is within reason, given that typical well bores extend more than 3218 m into the ground.

Unfortunately due to limited chemical resources it was only possible to experiment with a small range of samples. For this reason the trends developed above are not very reliable for predicting the load response of the "oilygel" in application. Regardless of the weak agreement of the trends developed for the "oilygel" to date, the experimental apparatus was successful in gathering reliable data for specimens made using the refined mixing methods. In order to develop more accurate trends for the load response for the "oilygel" it is necessary to conduct further testing making use of the optimized gelation and testing process. By increasing the amount of reliable data available it will be possible to increase the agreement of our theoretical trends with the experimental results allowing for a more accurate determination of the response of the "oilygel" under loading conditions.

In the future it will also be possible to employ the force transmission medium for testing of samples of higher lengths as the hydrostatic preloading associated with this testing method will not have a negative impact on the sample before applying a load with the load piston. Of course for this testing method it will be necessary to know the exact amount of fluid in the transmission medium to properly take into account the load already being exerted on the samples. By controlling the volume of transmission medium with the pipette dropper used for the transfer of chemicals during the gelation process it will be possible to know the volume of the medium to within ±0.005 ml reducing any error inherent with this methods of testing. This method would allow for the creation of a much more uniform load distribution over the sample reducing the creation of eccentric loads of the adhered area caused by the direct contact method. This method also provides a better approximation for the loading mechanism present for the proposed application.

Looking past static testing using the current experimental rig in the future it will be necessary to experiment with the "oilygel" in a dynamic flow situation. Due to the complexity of the mixing process this is key to understanding whether it is possible to create rigid plugs of "oilygel" in an

uncontrolled flow.   For the proposed application this would be integral to the success of the "oilygel" as a

well containment method.

6. References

[1]: Blount E. M. and E. Soeiinah, "Dynamic kill: Controlling wild wells a new way," World Oil, Oct. 1981, pp 109 126

[2]: Wessel, Michael and Bryan A. Tarr, "Underground well control: The key to drilling low-kick-tolerance wells safely and economically," SPE Drilling Engineering, p. 250, December 1991.

[3]: "Adhesion/Cohesion Theory." *Adhesives.org Home Page*. Jan. 2010. Web. 01 May 2011. <http://www.adhesives.org/StructuralDesign/AdhesionCohesionTheory.aspx>.[1]

[4]: Tadmor, Rafael. "The London–van Der Waals Interaction Energy between Objects of Various Geometrie." *Jounal of Physics*. Nov.-Dec. 2000. Web. May-June 2011. <http://dept.lamar.edu/chemicalengineering/www/Tadmor/papers/vanderWaalsforces/vdW1.pdf>.

[5]: "Mechanical Test Methods." *Adhesives Tool Kit*. Web. May-June 2011. <http://www.adhesivestoolkit.com/Docs/test/MECHANICAL%20TEST%20METHOD%201.xtp>.

[6]: Dillard, David A., and Alphonsus V. Pocius. *The Mechanics of Adhesion*. Amsterdam [u.a.: Elsevier, 2002. Print.

[7]: "Adhesive Testing Measurement Systems to Test Adhesive Strength, Dynamic Shear Strength, Adhesiblity, Peel Strength, Loop Tack and Other Qualities for Adhesives and Adhesive Products like Glues, Paints, Inks, Sealants, Glues, Tapes, Gels, Pastes, Resins, Waxes and Coatings." *Texture Technologies*. Web. 01 May 2011. <http://www.texturetechnologies.com/peel-strength/adhesive-testing-instruments.php?gclid=CPO52tW_x6gCFYXd4AodWlO5pg>.

[8]: "Shear Test Methods." *Adhesives Tool Kit*. Web. May-June 2011. <http://www.adhesivestoolkit.com/Docs/test/MECHANICAL%20TEST%20METHOD%201%20-%20Shear%20Tests.xtp#ref23>.

[9]: Brockmann, Walter, and Bettina Mikhail. *Adhesive Bonding Materials, Applications and Technology*. Weinheim: Wiley-VCH-Verl., 2009. Print.

[10]: "Tensile Test Methods." *Adhesives Tool Kit*. Web. May-June 2011. <http://www.adhesivestoolkit.com/Docs/test/MECHANICAL%20TEST%20METHOD%201%20-%20Tensile.xtp#_Toc109014538>.

[11]: Ita, Paul A., Mia Zaper, and Sean T. Socha. *Adhesives*. Cleveland: Freedonia Group, 1999. Print.

[12]: "T-Peel Test." *Adhesives Tool Kit*. Web. May-June 2011. " <http://www.adhesivestoolkit.com/Docs/test/MECHANICAL%20TEST%20METHOD%201%20-%20Tensile.xtp#_Toc109014538>.

7. Appendices

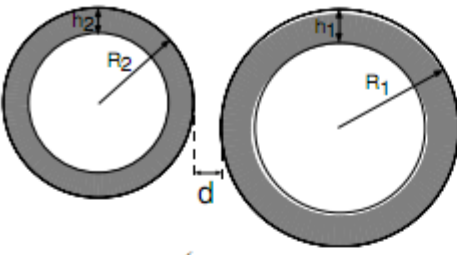### 7.1: Appendix A: Van der Waals Attraction between different Geometries
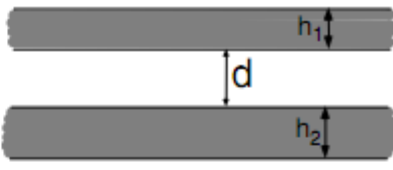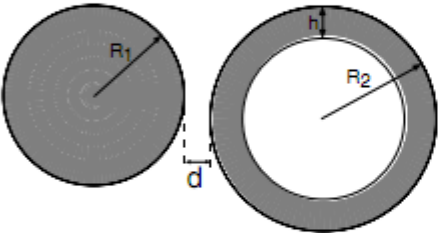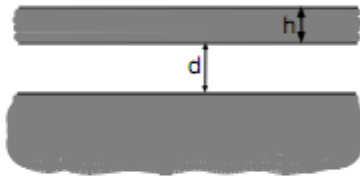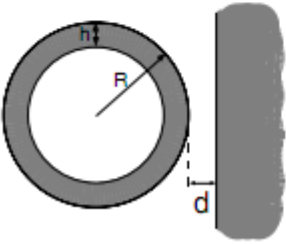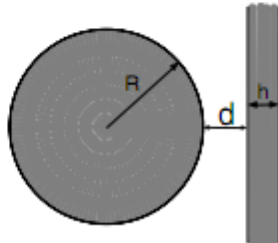
Two spherical shells	Two parallel walls
$$E = -\frac{AR_1 R_2}{6(R_1 + R_2)}\left(\frac{1}{(d+h_1+h_2)} - \frac{1}{(d+h_2)} - \frac{1}{(d+h_1)} + \frac{1}{d}\right) - \frac{A}{6}\ln\left[\frac{d(d+h_1+h_2)}{(d+h_1)(d+h_2)}\right]$$	$$E = -\frac{A}{12\pi}\left(\frac{1}{d^2} + \frac{1}{(d+h_1+h_2)^2} - \frac{1}{(d+h_1)^2} - \frac{1}{(d+h_2)^2}\right)$$ (per unit area)
A sphere and a spherical shell	**Thin and a semi infinite walls**
$$E = -\frac{AR_1 R_2}{6(R_1 + R_2)}\left(\frac{1}{d} - \frac{1}{(d+h)}\right) - \frac{A}{6}\ln\left[\frac{d}{(d+h)}\right]$$	$$E = -\frac{A}{12\pi}\left(\frac{1}{d^2} - \frac{1}{(d+h)^2}\right)$$ (per unit area)
Spherical shell and semi-infinite wall	**A sphere and a wall**
$$E = -\frac{AR}{6}\left(\frac{1}{d} - \frac{1}{(d+h)}\right) - \frac{A}{6}\ln\left[\frac{d}{(d+h)}\right]$$	$$E = -\frac{AR}{6}\left(\frac{1}{d} - \frac{1}{(d+h)}\right) - \frac{A}{6}\ln\left(\frac{d}{d+h}\right)$$

Figure A.1: A summary of the Van der Waals interactions between macroscopic objects.

46

7.2: Appendix B: *American Society for Testing and Materials Standards*: Adhesive Testing Methods Table

Test Method	Tensile Butt Joint	T-Peel	Climbing Drum	Floating Roller Method
Mechanical Properties Obtained	Tensile strength/modulus	Peel strength	Peel strength/skin stiffness	Peel strength
Material Quantity Requirements per specimen	Low	Low	High	Low
Typical Specimen Dimensions (mm)	Diameter 15–25 Adherend thickness 12–15	Bond length 150 Width 25 Adherend thickness 0.5–1.0 Arm length 50	Long adherend 300 Short adherend 240 Width 25 Adherend thickness 0.5–5.0	Flexible adherend 250 Rigid adherend 200 Width 25 Adherend thickness 0.5–1.6
Materials Suitable for Testing	1—6	1, 4 and 6 Flexible-flexible adherend	Flexible-rigid adherend 1—6 + sandwich structures	Flexible-rigid adherend 1—6
Cost of Specimen Fabrication/Preparation	Low	Low-moderate	High	Low—moderate
Cost of Testing/Specimen	Low	Low	Low—moderate	Low—moderate
Specimen Fabrication Equipment Requirements	Surface prepation	Surface preparation Bonding+Bonding jig	Surface preparation Bonding+Bonding jig	Surface preparation Bonding+Bonding jig
Specimen Instrumentation Requirements	Extensometer	None	None	Extensometer (2 off)
Test Equipment and Fixture Requirements	Universal test machine + end grips +	Universal test machine + end grips	Special test fixture Universal test machine + end grips	Special test fixtureUniversal test machine + end grips
Fatigue performance	Limited	unsuitable	Unsuitable	Unsuitable
Creep Performance	Suitable	Possibly	Unsuitable	Unsuitable
Environmental suitability	Suitable	Suitable	Unsuitable	Unsuitable
Data Reduction	Straightforward	Straightforward	Straightforward	Straightforward
Accuracy (Estimated)	To be determined	Large uncertainty (> 30%)	To be determined	To be determined
Standard Test Methods Available	ASTM D 897 ASTM D 2095 BS EN 26922	ISO 8510: Part 2 ISO 11339 ASTM 1876	BS 5350: Part C13 ASTM D 3167	ASTM D 3167

1 = metal-metal; 2 = metal-plastic; 3 = metal-composite; 4 = plastic-plastic; 5 = plastic-composite; 6 = composite-composite.

Figure A.2: Tensile and Peel Test methods used for adhesion testing and their respective ASTM Test Standardized Test Methods.

Test Method	Single-Lap	Double-Lap	V-Notched Beam	Arcan
Mechanical Properties Obtained	Shear strength	Shear strength	Shear strength/modulus	Shear strength/modulus
Material Quantity Requirements/Specimen	Low	Low	Low	Low
Typical Specimen Dimensions (mm)	Length 100 Width 25 Adherend thickness 2 Overlap length 25	Length 100 Width 25 Adherend thickness 12 Overlap length 25	Length 76 Width 20 Notch width 12 Adherend thickness 5	Length 52 Width 40 Notch width 12 Adherend thickness 6
Materials Suitable for Testing	1, 3 and 6	1, 3 and 6	1, 3 and 6	1, 3 and 6
Cost of Specimen Fabrication/Preparation	Low	Low-moderate	Moderate	Moderate
Cost of Testing/Specimen	Low	Low-moderate	Low-moderate	Low-moderate
Specimen Fabrication Equipment Requirements	Surface preparation Bonding + bonding jig	Surface preparation Bonding + bonding jig	Surface preparation Bonding + Bonding jig	Surface preparation Bonding + Bonding jig
Specimen Instrumentation Requirements	None	None	Shear extensometer Strain gauges	Shear extensometer Strain gauges
Test Equipment and Fixture Requirements	Universal test machine + loading grips	Universal test machine + loading grips	Universal test machine + loading fixture	Universal test machine + loading fixture
Fatigue performance	Limited	Suitable	Unuitable	Suitable
Creep Performance	Suitable	Possibly	Unsuitable	Unsuitable
Environmental suitability	Suitable	Suitable	Suitable	Suitable
Data Reduction	Straightforward	Straightforward	Straightforward	Straightforward
Accuracy (Estimated)	Moderate	Low (30%)	Low—moderate (10–20%)	Low—moderate (10–20%)
Standard Test Methods Available	BS 5350: Part C5 BS EN 1465 BS EN ISO 9664 ASTM D 1002 ASTM D 3166	BS 5350: Part C5 BS EN ISO 9664 ASTM D 1002 ASTM D 3166	No adhesive standard ASTM D 5379—PMCs	None

1 = metal-metal; 2 = metal-plastic; 3 = metal-composite; 4 = plastic-plastic; 5 = plastic-composite; 6 = composite-composite.

Figure A.3: Shear Test methods used for adhesion testing and their respective ASTM Test Standardized Test Methods.

7.3: Appendix C: "Oilygel" Formulations and Mixing Processes

Formulation Method #1:

Basic Recipe:
- 5 ml Silbond H5
- 5 ml APTES(3-Aminopropyltriethoxysilan)
- 5 ml ICTES(3-Isocyanatopropyltriethoxysilan)
- 2.1 g of 10W-40 Motor Oil(ρ=865kg/m^3)

Mixing Process #1:
- Mix the Silbond H5 with the Oil inside of the test section.
- Add Magnetic Stirring rod and place the test section of the magnetic stirrer and activate it at 1000rpm.
- Add the APTES to the mixture.
- Add the ICTES to the mixture wait 30 Sec and turn off the mixer.

Formulation Method #2:

Basic Recipe:
- 20 ml of Silbond H5
- 5ml of APTES
- 5ml of ICTES
- 2.1g of Oil

Mixing Process #2:
1) Mix the oil and the APTES (very miscible system) in a 500ml beaker.
2) Add the magnetic stirring rod.
3) Add the ICTES to the mixture, which causes a very exothermic reaction so this should be performed in the hood and stir at 1000rpm for 30 sec.
4) Add the Silbond H5.
5) Gelation should take around 1 min 10 sec to solidify after the addition of Silbond H5, in order to allow transfer time from glassware to the test section.
6) Transfer should take place around 45 sec after the addition of the Silbond H5.
7) Wait 4 min before performing mechanical tests.

Formulation Method #3

Basic Recipe
- 20 ml of Silbond H5
- 7.5ml of APTES
- 7.5ml of ICTES
- 2.1g of Oil

Mixing Process #3:
1) Mix the oil and the APTES(very miscible system) in a 500ml beaker.
2) Add magnetic stirring rod and place it on the magnetic stirrer.
3) Add the ICTES to the mixture, which causes a very exothermic reaction so this should be performed in the hood and stir at 1000rpm for 30 sec.
4) Add the Silbond H5.
5) Gel should take around 50 sec to solidify after the addition of Silbond H5 to allow transfer time from glassware to the test section.
6) Transfer should take place around 30 sec after the addition of the Silbond H5.
7) Wait 3 min before performing mechanical tests.

Formulation #1 Recipes

Sample Length(cm)	2.54	5.08	7.62	10.16	12.7
Sample Diameter(cm)	2.54	2.54	2.54	2.54	2.54
Sample Volume(ml)	51.481	102.963	154.444	205.926	257.407
Required Silbond H5 (ml)	6.026	12.052	18.078	24.104	30.129
Required Oil(ml)	2.926	5.852	8.778	11.703	14.629
Required Oil(g)	2.531	5.062	7.593	10.123	12.654
Required APTES(ml)	6.026	12.052	18.078	24.104	30.129
Required ICTES(ml)	6.026	12.052	18.078	24.104	30.129

Formulation #2 Recipes

Sample Length(cm)	2.54	5.08	6.35	7.62	12.7
Sample Diameter(cm)	2.54	2.54	2.54	2.54	2.54
Sample Volume(ml)	51.481	102.963	128.704	154.444	257.407
Required Silbond H5 (ml)	13.632	27.264	34.080	40.896	68.161
Required Oil(ml)	1.655	3.310	4.137	4.964	8.274
Required Oil(g)	1.431	2.863	3.578	4.294	7.157
Required APTES(ml)	3.408	6.816	8.520	10.224	17.040
Required ICTES(ml)	3.408	6.816	8.520	10.224	17.040

Formulation #3 Recipes

Sample Length(cm)	2.54	5.08	7.62	10.16	12.7
Sample Diameter(cm)	2.54	2.54	2.54	2.54	2.54
Sample Volume(ml)	51.481	102.963	154.444	205.926	257.407
Required Silbond H5 (ml)	11.908	23.816	35.723	47.631	59.539
Required Oil(ml)	1.445	2.891	4.336	5.782	7.227
Required Oil(g)	1.250	2.501	3.751	5.001	6.252
Required APTES(ml)	4.465	8.931	13.396	17.862	22.327
Required ICTES(ml)	4.465	8.931	13.396	17.862	22.327

7.4: Appendix D: Apparatus Design Drawings and Materials Selection Table

Figure A.3: Schematic of the Load Piston.

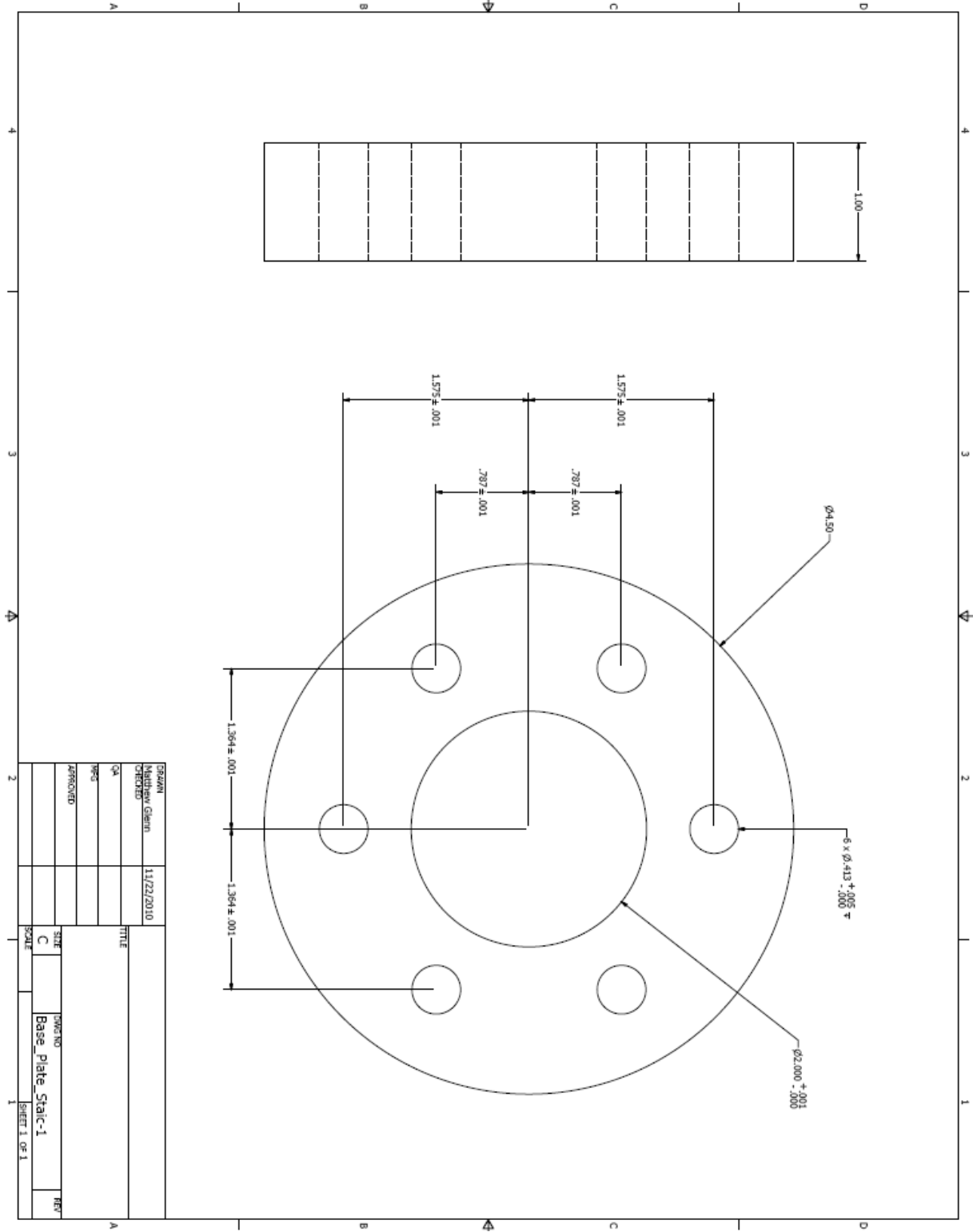Figure A.4: Schematic of the Alignment Plate.

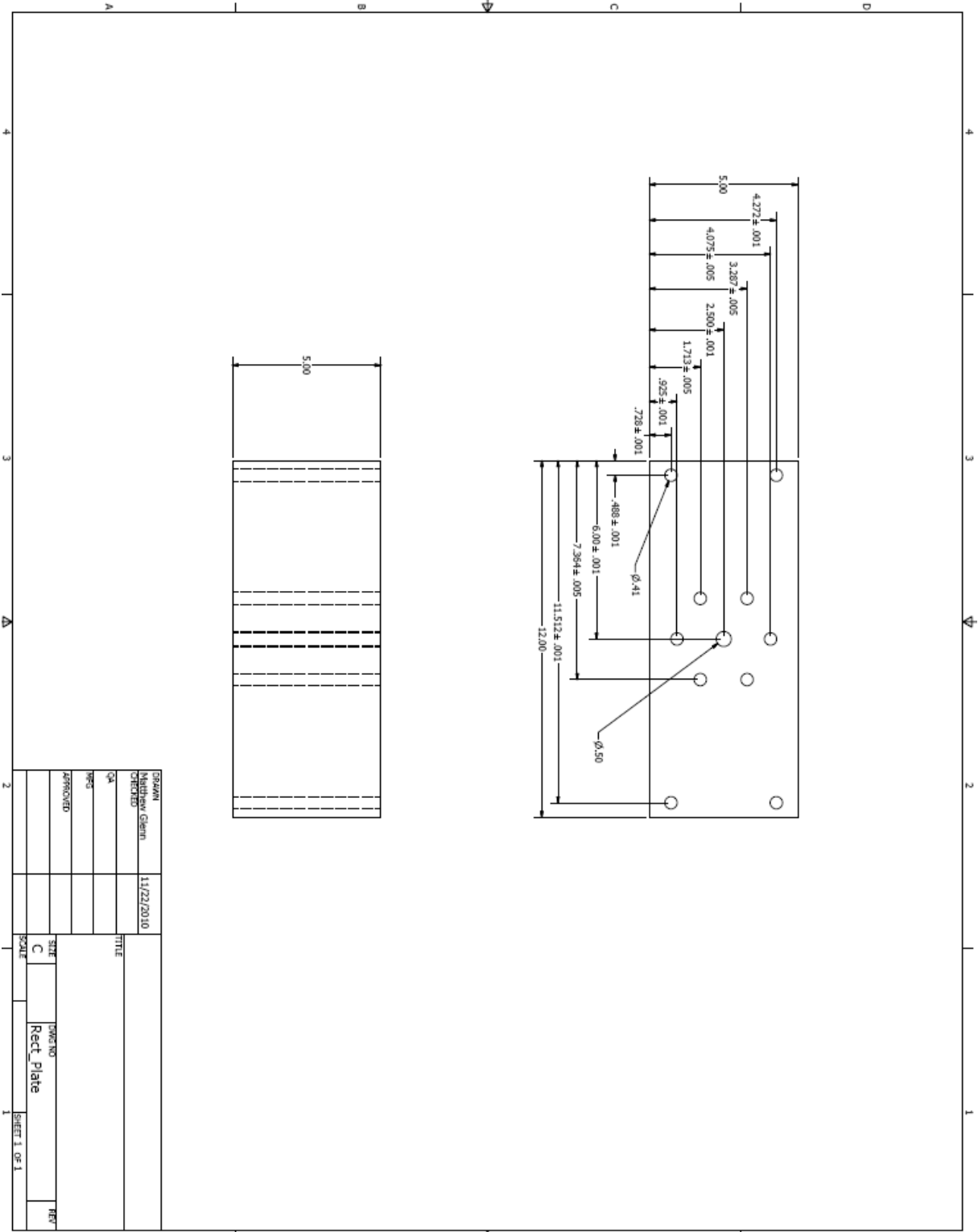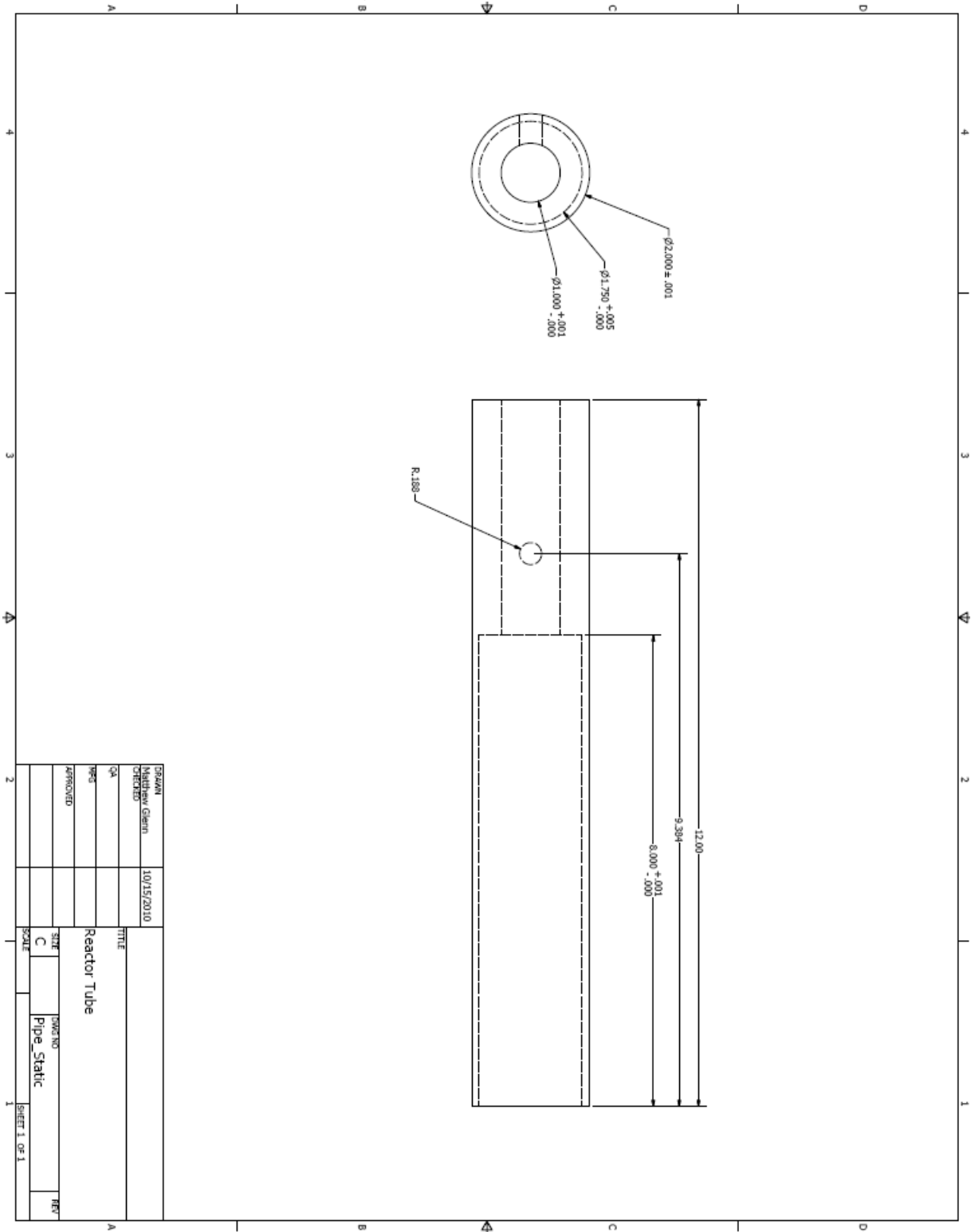**Figure A.4: Schematic of the Anti-Deflection Plate.**

Figure A.5: Schematic of the Test Section Housing.

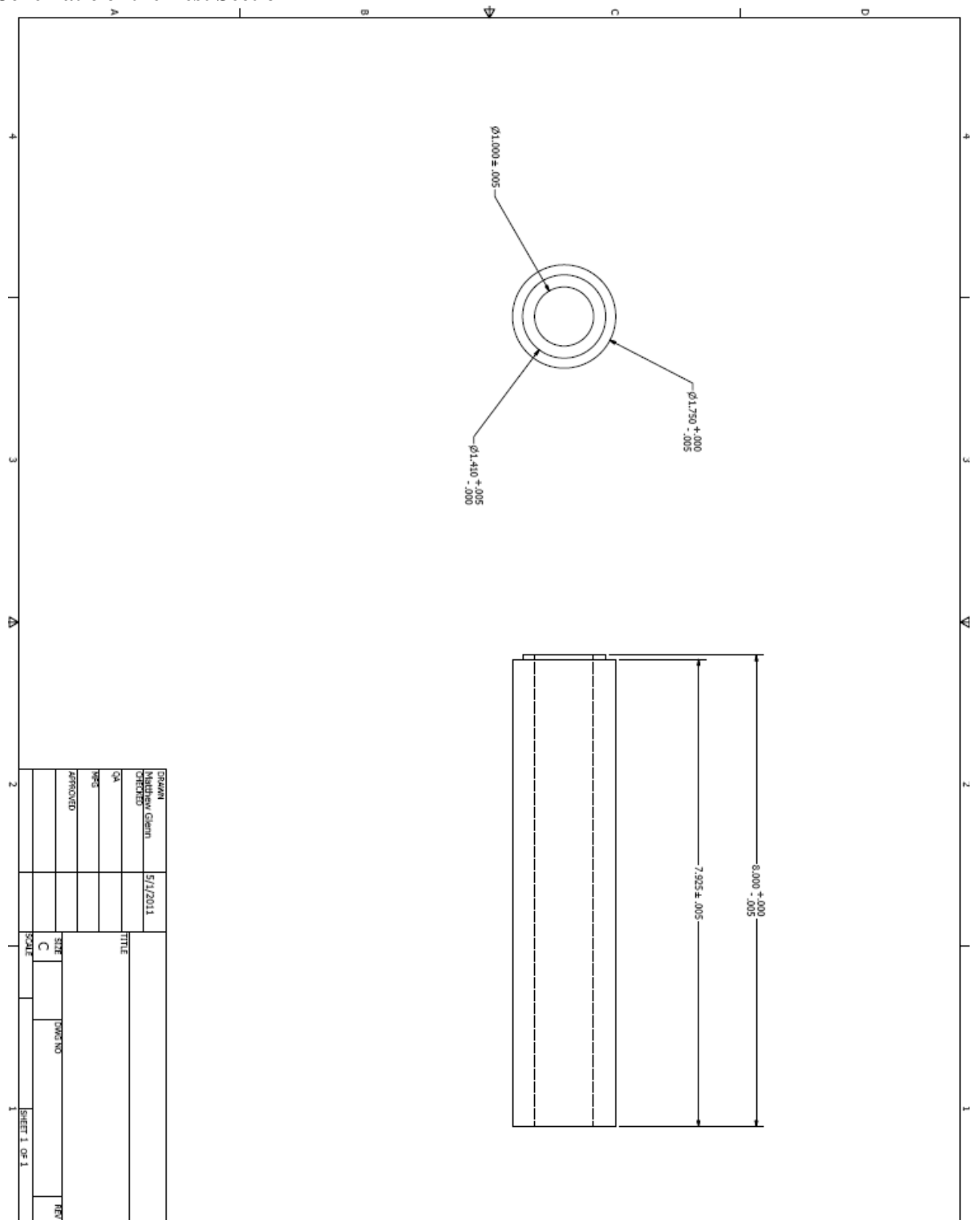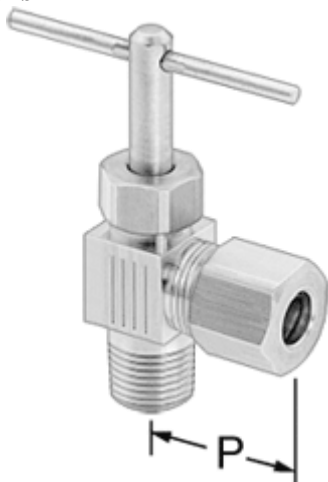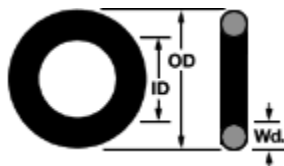**Figure A.6: Schematic of the Test Section**

Figure A.7: Elbow Valve Specifications

Brass Elbow Needle Valve 3/8" NPTF Male Pipe X 1/4" Tube Connections
☐ Max. Pressure for Water, Oil, and Inert Gas: 150 psi @250° F
☐ Temp. Range: -45° to +250° F

Figure A.8: O-ring Specifications

Static O-ring: AS568A-129

Type	O-Ring
O-Ring Type	Standard
Cross Section Shape	Round
Width	3/32"
Actual Width	.103"
Inside Diameter	1-9/16"
Actual Inside Diameter	1.549"
Outside Diameter	1-3/4"
Actual Outside Diameter	1.755"
Material	Polyurethane
Polyurethane Type	Standard
Durometer	Hard
Durometer Shore	Shore A: 70
Temperature Range	-20° to +180°F
Color	Black
Specifications Met	Not Rated

Dynamic O-Ring: AS568A-022

Type	O-Ring
O-Ring Type	Standard
Cross Section Shape	Round
Width	1/16"

Actual Width	.070"
Inside Diameter	1"
Actual Inside Diameter	.989"
Outside Diameter	1-1/8"
Actual Outside Diameter	1.129"
Material	Polyurethane
Polyurethane Type	Standard
Durometer	Hard
Durometer Shore	Shore A: 70
Temperature Range	-20° to +180°F
Color	Black
Specifications Met	Not Rated

Figure A.9: Component Material List

Part	Material	McMaster Part #
Load Piston	Stainless Steel 304	8934K211
Anti-Deflection Plate	Alloy 6061	9008K741
Alignment Plate	Alloy 6061	9246K61
Test Section Housing	Alloy 6061	9056K151
Test Section	Low Carbon-Steel	7767T791
Dynamic O-Ring	Polyurethane	9558K59
Static O-Ring	Polyurethane	9558K94

7.5: Appendix E: Instron Load Cells

Model: 2530-427

Capacity	0.1 kN (10 kgf, 22 lbf)
Mechanical Fitting	2.5 and 6 mm clevis pin (Type OOf and Of)
Accessory Diameter	85 mm (3.3 in)
Upper Effective Length	48 mm (1.9 in)
Static or Fatigue Rated	Static

Model: 2530-426

Capacity	1 kN (100 kgf, 225 lbf)
Mechanical Fitting	6 mm clevis pin (Type Of)
Accessory Diameter	85 mm (3.3 in)
Upper Effective Length	54 mm (2.1 in)
Static or Fatigue Rated	Static

Model: 2530-443

Capacity	10 kN (1000 kgf, 2250 lbf)
Mechanical Fitting	6 mm clevis pin (Type Of)
Accessory Diameter	107 mm (4.2 in)
Upper Effective Length	97.5 mm (3.8 in)
Static or Fatigue Rated	Static